Molecular Pharmacology Fast Forward. Published on October 17, 2016 as DOI: 10.1124/mol.116.106112
This article has not been copyedited and formatted. The final version may differ from this version.

Title Page

Discovery and characterization of novel GPR39 agonists allosterically modulated by zinc

Seiji Sato, Xi-Ping Huang, Wesley K. Kroeze and Bryan L. Roth

Department of Pharmacology (SS, X-PH, WKK and BLR) and National Institute of Mental Health Psychoactive Drug Screening Program (NIMH PDSP; X-PH and BLR) School of Medicine, University of North Carolina at Chapel Hill, Chapel Hill, NC

Molecular Pharmacology Fast Forward. Published on October 17, 2016 as DOI: 10.1124/mol.116.106112
This article has not been copyedited and formatted. The final version may differ from this version.

Running Title Page

Running Title:

Novel agonists of the GPR39 zinc receptor

Corresponding author:

Bryan Roth

Address: Genetic Medicine Building Rm 4072, 120 Mason Farm Rd, Chapel Hill, NC 27599

Phone: 919-966-7535

Fax: 919-843-5788

E-mail: bryan_roth@med.unc.edu

Number of text pages: 35

Number of tables: 8

Number of figures: 8

Number of references: 56

Number of words in Abstract: 132

Number of words in Introduction: 511

Number of words in Discussion: 1496

Molecular Pharmacology Fast Forward. Published on October 17, 2016 as DOI: 10.1124/mol.116.106112
This article has not been copyedited and formatted. The final version may differ from this version.

List of abbreviations:

Ala, Alanine; BRET, Bioluminescence resonance energy transfer; BSA, Bovine serum Albumin; CXCR7, C-X-C chemokine receptor type 7; DMEM, Dulbecco's modified Eagle medium; DMSO, Dimethyl sulfoxide; ELISA, Enzyme-linked immunosorbent assay; FBS, Fetal bovine serum; GHSR, Growth hormone secretagogue receptor; GPCR, G-protein coupled receptor; GPRC6A, G-protein coupled receptor family C group 6 member A; GPR39-C3, N-[3-Chloro-4-[[[2-(methylamino)-6-(2-pyridinyl)-4-pyrimidinyl]amino]methyl]phenyl]methanesulfonamide; GSK2636771, 1H-Benzimidazole-4-carboxylic acid, 2-methyl-1-[[2-methyl-3-(trifluoromethyl)phenyl]methyl]-6-(4-morpholinyl)-; HBSS, Hank's balanced salt solution; HEK293T, Human embryonic kidney 293T; His, Histidine; HRP, Horseradish peroxidase; HTLA, HEK293-derived cell line containing stable integrations of a tTA-dependent luciferase reporter and a β-arrestin2-TEV fusion gene; HTR1A, 5HT-1A receptor; IBMX, 3-Isobutyl-1-methylxanthine; JAK2, Janus activating kinase 2; LY2784544, 3-(4-chloro-2-fluorobenzyl)-2-methyl-N-(3-methyl-1H-pyrazol-5-yl)-8-(morpholinomethyl)imidazo[1,2-b]pyridazin-6-amine; MLNR, Motilin receptor; MTLNR1A, Melatonin receptor 1A; NMUR1, Neuromedin U receptor1; NMUR2, Neuromedin U receptor2; NTSR1, Neurotensin receptor 1; NTSR2, Neurotensin receptor2; PAM, Positive allosteric modulator; PI3Kβ, Phosphoinositide 3-kinase beta; PTEN, Phosphatase and tensin homolog deleted from chromosome 10; RLU, relative luminescence units; TEV, Tobacco etch virus protease; tTA, Tetracycline transactivator.

Molecular Pharmacology Fast Forward. Published on October 17, 2016 as DOI: 10.1124/mol.116.106112
This article has not been copyedited and formatted. The final version may differ from this version.

Abstract

In this study, we identified two previously described kinase inhibitors-- LY2784544 and GSK2636771-- as novel GPR39 agonists by unbiased small-molecule-based screening using a β–arrestin recruitment screening approach (PRESTO-Tango). We characterized the signaling of LY2784544 and GSK2636771 and compared their signaling patterns with a previously described “GPR39-selective” agonist GPR39-C3 at both canonical and non-canonical signaling pathways. Unexpectedly, all three compounds displayed probe-dependent and pathway-dependent allosteric modulation by concentrations of zinc reported to be physiological. The potencies of LY2784544 and GS2636771 at GPR39 in the presence of zinc were generally as potent or more potent than their reported activities against kinases in whole cell assays. These findings reveal an unexpected role of zinc as an allosteric potentiator of small-molecule-induced activation of GPR39 and expand the list of potential kinase off-targets to include under-studied GPCRs.

Molecular Pharmacology Fast Forward. Published on October 17, 2016 as DOI: 10.1124/mol.116.106112
This article has not been copyedited and formatted. The final version may differ from this version.

Introduction

G protein-coupled receptors (GPCRs) transduce extracellular stimuli into intracellular signals, have crucial roles in virtually all of human physiology, and are the targets for about one-third of currently marketed drugs (Overington *et al.*, 2006; Rask-Andersen *et al.*, 2014). When agonists bind to GPCRs, signals are transduced into cells via a number of Gα proteins, or β-arrestins and other interacting proteins. In the human genome, there are about 350 non-olfactory GPCRs, of which about 100 are still orphans, *i.e.,* their endogenous ligands are yet unknown (Vassilatis *et al.*, 2003; Fredriksson and Schiöth, 2005; Bjarnadóttir *et al.*, 2006; Regard *et al.*, 2008; Komatsu *et al.*, 2014; Roth and Kroeze, 2015) or alternatively, they are very poorly annotated with respect to ligands, whether endogenous or surrogate. In the current study, we report on the discovery of novel surrogate ligands for GPR39, previously described as a zinc receptor (Holst *et al.*, 2007).

GPR39 is a member of the ghrelin peptide receptor family. Although the ligands of the non-orphan receptors in this family are all peptides (ghrelin, GHSR, Kojima *et al.*, 1999; neurotensin, NTSR1 and NTSR2, Tanaka *et al.*, 1990, Vita *et al.*, 1998; motilin, MLNR, Feighner *et al.,* 1999; neuromedin U, NMUR1 and NMUR2, Kojima *et al.,* 2000; Bhattacharyya *et al.,* 2004), GPR39 has been reported to be a Zn^{2+} metal ion-sensing receptor (Holst *et al.*, 2007). Other divalent metal ions, such as Ni^{2+}, Cd^{2+}, Cr^{2+} and Fe^{2+}, have also been reported to activate GPR39 (Holst *et al.*, 2007; Huang *et al.,* 2015). GPR39 is widely expressed in several organs, including the gastrointestinal tract, pancreas, thyroid, brain and others (Popovics and Stewart, 2011).

Molecular Pharmacology Fast Forward. Published on October 17, 2016 as DOI: 10.1124/mol.116.106112
This article has not been copyedited and formatted. The final version may differ from this version.

GPR39 has been reported to be associated with type 2 diabetes (Holst *et al.*, 2009; Verhulst *et al.*, 2011) and depression (Młyniec and Nowak, 2015; Młyniec, Gaweł, and Nowak, 2015; Młyniec, Gaweł, Librowski, *et al.*, 2015; Młyniec, Singewald, *et al.*, 2015). GPR39 has been found to be expressed in mouse intestinal fibroblast-like cells (Zeng *et al.*, 2012), human colon adenocarcinoma HT-29 cells (Yasuda et al., 2007; Cohen, Azriel-Tamir, *et al.*, 2012; Boehm *et al.*, 2013; Cohen *et al.*, 2014), rat colon BRIN-BD11 cells (Moran *et al.*, 2015) and mouse pancreatic epithelial NIT-1 cells (Fjellström *et al.*, 2015). All of these cell types respond to Zn^{2+} via various signal transduction pathways. Early studies reported the peptide obestatin to be a GPR39 agonist (Zhang, 2005), but subsequent work failed to reproduce these results (Lauwers *et al.*, 2006; Holst *et al.*, 2007; Zhang *et al.*, 2007). Zn^{2+} stimulates signaling via the Gq and β-arrestin pathways, as well as the Gs pathway (Holst *et al.*, 2007). Recently, three groups have reported small molecule agonists for GPR39 (Boehm *et al.*, 2013; Peukert *et al.*, 2014; Fjellström *et al.*, 2015). However, the signaling pathways induced by these agonists, and their relationship to Zn^{2+} concentrations, remain to be elucidated. Additionally, the physiological significance of each GPR39 signaling pathway remains unclear. Here we provide an approach for discovering new GPR39 agonists useful for illuminating GPR39 signaling pathways. We exemplify two compounds and elucidate how their signaling is allosterically modulated by Zn^{2+}.

Molecular Pharmacology Fast Forward. Published on October 17, 2016 as DOI: 10.1124/mol.116.106112
This article has not been copyedited and formatted. The final version may differ from this version.

Materials and Methods

Compounds

The following libraries were screened in quadruplicate using a modified TANGO β–arrestin recruitment assay (Barnea *et al.*, 2008; Kroeze *et al.*, 2015) for activity at GPR39: NCC-1 [National Clinical Collection – 446 compounds], NIMH X-901 [271 compounds], Prestwick [1120 compounds], Tocris [1280 compounds], Selleck [Selleckchem – 1836 compounds] and Spectrum [Microsource – 2400 compounds] at a final concentration of 10 μM, following the previously published method (Kroeze *et al.,* 2015). Daughter libraries were prepared and kept at -20C until use. LY2784544, GSK2636771, GPR39-C3 and obestatin were obtained from Selleckchem, MedChem Express, Xcessbio and Sigma, respectively.

Site-directed mutagenesis

The His17Ala/His19Ala mutation in GPR39 was introduced using the GPR39-TANGO construct (Kroeze *et al.,* 2015) as a template, PrimeSTAR Max (TAKARA Clontech) as the polymerase and the following primers: [39T-H17AH19A_S; 5'-GACGCTAGCGCTGTGCCGGAGTTTGAAGTGGC -3', 39T-H17AH19A_A; 5'-CACAGCGCTAGCGTCAATAATCTGGCTACAGT-3']. Mutations were confirmed by sequencing (Eton Bioscience Inc., Research Triangle Park, NC, USA). For assessment of G-protein-mediated signaling, GPR39-TANGO constructs were "de-TANGO-ized" by introduction of a stop codon immediately following the GPR39 open reading frame using the following primers: [TangoUniStopCleanF : 5'-

Molecular Pharmacology Fast Forward. Published on October 17, 2016 as DOI: 10.1124/mol.116.106112
This article has not been copyedited and formatted. The final version may differ from this version.

GACGCACCTAGCTCGAGTCTAGAGGGCCCG-3', TangoUniStopCleanR : 5'-CTCGAGCTAGGTGCGTCCACCGGTATCGAT-3'] , and also confirmed by sequencing.

TANGO assay

HTLA cells (a HEK293 cell line stably expressing a tTA-dependent luciferase reporter and a β-arrestin2-TEV fusion gene) were a gift from the laboratory of R. Axel (Columbia Univ.) and were maintained in DMEM supplemented with 10% fetal bovine serum (FBS), 100 U/ml penicillin and 100 µg/ml streptomycin, 2 µg/ml puromycin and 100 µg/ml hygromycin B in a humidified atmosphere at 37°C in 5% CO_2. TANGO β-arrestin recruitment assays were carried out as described by Kroeze *et al.* (2015). All experiments were done in quadruplicate. Results expressed as relative luminescence units (RLU) were exported into Excel spreadsheets, and analyses were done using Graphpad Prism. In order to calculate fold-change, wells without compounds and without Zn^{2+} were used as "basal"; results were finally expressed as $\log_2$ fold-change.

PRESTO-Tango GPCR-ome Profiling

The PRESTO-Tango GPCR-ome assay was performed as previously described (Kroeze *et al.*, 2015). HTLA cells were cultured in poly-L-Lys-coated 384-well white clear-bottom cell culture plates (Greiner) in DMEM supplemented with 10% dialyzed FBS at a density of 10,000 cells/well in a total volume of 50 µl one day before transfection. The next day, 40 ng/well DNA was transfected into each well using the calcium phosphate precipitation method. The following day, the medium was aspirated from the plate and replaced with 50 µL/well fresh DMEM containing 1% dialyzed FBS

Molecular Pharmacology Fast Forward. Published on October 17, 2016 as DOI: 10.1124/mol.116.106112
This article has not been copyedited and formatted. The final version may differ from this version.

and 100 μM $ZnCl_2$, with 1 μM compound or without compound, and incubated overnight. DRD2 and 1 μM quinpirole were set on every plate as a positive control for this assay. The detection step was performed using the method described by Kroeze *et al.* (2015). All experiments were done in quadruplicate. Results expressed as relative luminescence units (RLU) were exported into Excel spreadsheets, and analyses were done using Graphpad Prism. The mean fold-change for each receptor was calculated as (mean RLU with ligand/mean RLU without ligand).

Inositol phosphate accumulation assay

Inositol phosphate accumulation assays were performed as in previous reports (https://pdspdb.unc.edu/pdspWeb/content/PDSP%20Protocols%20II%202013-03-28.pdf; Storjohann *et al.*, 2008). HEK293T cells were maintained in DMEM supplemented with 10% FBS, 100 U/ml penicillin, and 100 μg/ml streptomycin. Cells were transfected with 20 μg of receptor DNA per 15-cm cell-culture dish and incubated overnight at 37°C in a humidified 5% CO_2 incubator. The next day, 30,000 cells/well were seeded into poly-L-lysine–coated 96-well plates in 100 μl per well of DMEM supplemented with 10% dialyzed FBS, 100 U/ml penicillin and 100 μg/ml streptomycin. After attaching to the plate, cells were incubated for 16 h as above in inositol-free DMEM (United States Biological) containing 10% dialyzed FBS, and 1 μCi/well of *myo*-[^{3}H]inositol (Perkin Elmer). On the following day, cells were washed with 100 μl drug buffer (1× HBSS, 24 mM $NaHCO_3$, 11 mM glucose, and 15 mM LiCl, pH 7.4) and treated with 100 μl of drug buffer containing drug and 0.3% bovine serum albumin (BSA;

Molecular Pharmacology Fast Forward. Published on October 17, 2016 as DOI: 10.1124/mol.116.106112
This article has not been copyedited and formatted. The final version may differ from this version.

Sigma) in quadruplicate for 1 h at 37°C in a 5% CO_2 incubator. After treatment, drug solution was removed by aspiration, and 40 µl of 50 mM formic acid was added to lyse cells for 30 min at 4°C. After cell lysis, 20 µl of the acid extract was transferred to each well of a polyethylene terephthalate 96-well sample plate (PerkinElmer, 1450-401) and mixed with 75 µl of PerkinElmer RNA Binding YSi SPA Beads (RPNQ0013) at a concentration of 0.2 mg beads/well and incubated for 30 min at room temperature. Bead/lysate mixtures were then counted with a Microbeta Trilux counter. Data were exported into Excel spreadsheets and analyzed using Graphpad Prism.

cAMP accumulation assay

Receptor-mediated Gs pathway signaling was measured using a split-luciferase receptor assay (GloSensor cAMP assay, Promega). In brief, HEK293T cells were transiently co-transfected with receptor DNA and the GloSensor cAMP reporter plasmid (GloSensor 7A). The following day, transfected cells were plated into poly-L-lysine-coated 384-well white clear-bottom cell culture plates in DMEM supplemented with 1% dialyzed FBS (Omega Scientific), 100 U/ml penicillin and 100 µg/ml streptomycin at a density of 15,000 cells/well in a total volume of 40 µl. The next day, culture medium was removed by aspiration, and cells were incubated with 20 uL of 4 mM luciferin (GoldBio, St. Louis, MO, USA) prepared in drug buffer (20 mM HEPES, 1× HBSS and 0.3 % BSA, pH 7.4) for 30 min at 37°C. Next, cells were incubated with 10 µl of a 3x concentration of drug at room temperature for 15 min. Following drug treatment, cells were incubated with 10 µl of a 4x concentration of $ZnCl_2$ solution in drug buffer, or drug buffer alone, for 15 min at room temperature. Luminescence was then counted using a Microbeta Trilux

Molecular Pharmacology Fast Forward. Published on October 17, 2016 as DOI: 10.1124/mol.116.106112
This article has not been copyedited and formatted. The final version may differ from this version.

luminescence counter (Perkin Elmer). All experiments were performed in quadruplicate, and exported into Excel spreadsheets, which were then analyzed using Graphpad Prism. In order to calculate fold-change, wells without compounds and without Zn^{2+} were used as "basal".

Cell ELISA

To confirm cell surface expression of the FLAG-tagged GPR39 and its mutants, immunohistochemistry was done using cells plated into 384-well plates as above at 10,000 cells/well. Cells were fixed with 20 µl/well 4% para-formaldehyde for 10 min at room temperature. After fixation, cells were washed twice with 40 µl/well of PBS at pH7.4. Blocking was done with 20 µl/well of 5% normal goat serum in PBS for 30 min at room temperature. After blocking, 20 µl/well of anti-FLAG-HRP conjugated antibody (Sigma) diluted 1/10,000 was added and incubated for 1 h at room temperature. This was followed by two washes with 80 µl/well PBS. Then, 20 µl/well of SuperSignal ELISA Pico Substrate (Sigma) was added and luminescence was counted using a Microbeta Trilux luminescence counter. Expression of mutants was normalized by using expression of wildtype receptors as 100% and untransfected cells as 0%. As previously, all experiments were done in quadruplicate.

FLIPR assay

HT-29 (ATCC) and PC-3 (obtained from Kim Lab, The Lineberger Comprehensive Cancer Center at UNC Chapel Hill) were maintained in 10% FBS, McCoy's 5A medium (Gibco) and 10% FBS, DMEM respectively. The cells were seeded into poly-L-Lys-

Molecular Pharmacology Fast Forward. Published on October 17, 2016 as DOI: 10.1124/mol.116.106112
This article has not been copyedited and formatted. The final version may differ from this version.

coated 384-well black clear-bottom cell culture plates in each medium supplemented with 10% dialyzed fetal bovine serum at a density of 10,000 cells/well in a total volume of 50 µl one day before assay. The following day, medium was discarded and cells were loaded with 20 µl/well of 1x Fluo-4 Direct Calcium dye (20 mM HEPES, 1x HBSS, 2.5 mM Probenecid, pH 7.40). Plates were incubated for 60 min at 37°C. The FLIPR was programmed to take 10 readings (1 read per second) first as a baseline before addition of 10 μl of 3x drug solutions. The fluorescence intensity was recorded for 2 minutes after drug addition.

Molecular Pharmacology Fast Forward. Published on October 17, 2016 as DOI: 10.1124/mol.116.106112
This article has not been copyedited and formatted. The final version may differ from this version.

RESULTS

Discovery of novel GPR39 agonists

The TANGO β-arrestin recruitment assay was used to screen several compound libraries (Methods), which totaled approximately 5000 unique compounds, for agonist activity at GPR39 in the absence of Zn^{2+}. Approximately 20 compounds showed activities over two-fold higher than basal (*i.e.,* $\log_2$ fold-change >1) (Fig. 1A); after exclusion of promiscuous compounds that also activated other GPCR targets (data not shown), the JAK2 inhibitor LY2784544 and the PI3K beta inhibitor GSK2636771 were identified as GPR39 agonists (Fig. 1A). The structures of these compounds are similar to each other, but markedly different from the GPR39-C3 compound that has previously been reported to be an agonist at GPR39 (Fig. 1B; Peukert *et al.,* 2014). When tested at 11 other GPCRs, neither of these compounds showed agonist activity (Fig. 1C). Additionally, we also tested obestatin, which has previously been reported to be a GPR39 agonist (Zhang, 2005), for activity at GPR39 and found it to be inactive (Supplementary Fig. 1A); we then tested obestatin for activity at 320 GPCRs using the Presto-TANGO method (Kroeze *et al.,* 2015; Manglik *et al.,* 2016), and found it to be inactive at all targets tested (Supplementary Fig. 1B), both in the presence and absence of Zn^{2+}. Additionally, we performed a GPCR-ome analysis (Kroeze *et al.,* 2015; Manglik *et al.,* 2016) for all of three GPR39 agonist compounds, *i.e.,* GPR39-C3, LY2784544 and GSK2636771. At 1 μM concentrations, and in the presence of 100 μM $ZnCl_2$, each compound showed obvious activity at only one receptor in addition to GPR39 - HTR1A by GPR39-C3, MTLNR1A by LY2784544, CXCR7 by GSK2636771, respectively (Fig.

Molecular Pharmacology Fast Forward. Published on October 17, 2016 as DOI: 10.1124/mol.116.106112
This article has not been copyedited and formatted. The final version may differ from this version.

2A-C). Thus, these compounds are highly specific agonists at GPR39. These activities were subsequently confirmed with concentration-response curves (Supplementary Fig. 2).

Allosteric modulation of GPR39 β-arrestin recruitment activity

Since Zn^{2+} had previously been reported to be an agonist at GPR39, and it because it seemed unlikely that these compounds might be interacting at the zinc site, we wondered if zinc allosterically modulated the GPR39 agonist activity of small molecules. We used the previously reported GPR39 agonist GPR39-C3 (Peukert *et al*., 2014), as well as the two compounds discovered in our screens, LY2784544 and GSK2636771 (Fig. 1), at various concentrations of Zn^{2+} in the TANGO assay (Fig. 3). Zn^{2+} alone showed very little activity in this assay (Fig. 3D). However, all three compounds showed a Zn^{2+}-dependent increase in potency and efficacy up to a Zn^{2+} concentration of 100 μM (Fig. 3A-C); at a Zn^{2+} concentration of 316 μM, no activity was seen, presumably due to the toxic effects of Zn^{2+} at such high concentrations. In an attempt to determine whether responses to Zn^{2+} could be seen with shorter exposures to its potentially toxic effects, we exposed GPR39-expressing HTLA cells to Zn^{2+} for various times, followed by a washout, and continued incubation overnight; longer exposures to higher concentrations of Zn^{2+} were apparently toxic to cells, but significant β-arrestin recruitment activity was not seen at any concentration, or with any length of exposure (Fig. 3D). The efficacy and potency values for these three compounds at various Zn^{2+} concentrations are shown in Table 1; all three compounds showed E_{max} values between 20- and 30-fold

Molecular Pharmacology Fast Forward. Published on October 17, 2016 as DOI: 10.1124/mol.116.106112
This article has not been copyedited and formatted. The final version may differ from this version.

above basal at 100 μM Zn^{2+}. Interestingly, GPR39-C3 showed marked activity in the absence of Zn^{2+}, whereas LY2784544 and GSK2636771 had minimal or no activity in the absence of zinc. Taken together, the results shown in Table 1 indicate that Zn^{2+} acts as a positive allosteric modulator (PAM) of the activity of GPR39-C3 in terms of efficacy only, whereas Zn^{2+} was a PAM for the activities of LY2784544 and GSK2636771 in terms of **both** efficacy and potency. It should be noted that all three compounds were apparently toxic to HTLA cells at high concentrations, and therefore data from these high concentrations were excluded from this analysis. We also tested whether LY2784544 could act as an antagonist to the GPR39-C3 response at various Zn^{2+} concentrations, and found that LY2784544 did not antagonize the GPR39-C3 response (Supplementary Fig. 3). Together, our results suggest that Zn^{2+} stabilizes a conformation of GPR39 that can be further activated to recruit β–arrestin by LY2784544. In addition, Ni^{2+} was also shown to be an agonist of GPR39 in β-arrestin recruitment activity (Fig. 4), as had previously been reported using a BRET assay (Holst *et al.*, 2007).

Allosteric modulation of GPR39 Gq-mediated signaling

We also measured GPR39-mediated Gq pathway signaling using a PI hydrolysis assay. As can be seen in Fig. 4A-C, all three tested compounds stimulated Gq signaling. The Zn^{2+} dependence of responses to LY2784544 (Fig. 4B) and GSK2636771 (Fig. 4C) was much greater than that of GPR39-C3 (Fig. 4A), *with leftward shifts of more than 1000-fold* compared to less than 10-fold for GPR39-C3. At the higher Zn^{2+} concentrations, all

Molecular Pharmacology Fast Forward. Published on October 17, 2016 as DOI: 10.1124/mol.116.106112
This article has not been copyedited and formatted. The final version may differ from this version.

three compounds were much more potent with respect to Gq signaling (Fig. 4A-C) than they were in β-arrestin recruitment (Fig. 3), showing EC_{50} values in the low nanomolar range (Table 2). The allosteric parameters were calculated according to Black-Leff Ehlert model (Kenakin, 2012). The allosteric modulator efficacy values τ_B were greater than 0, indicating that Zn^{2+} is PAM agonist (Fig. 4B and C). All three compounds showed a maximal efficacy of three-to-four-fold over basal (Table 2). The maximal efficacy of all three compounds at GPR39 in Gq signaling was not affected by Zn^{2+} concentration (Fig. 4A-C; Table 2), although Zn^{2+} and Ni^{2+} stimulated GPR39-mediated Gq signaling on their own (Fig. 4D-F; Table 3). Interestingly, the potency of Ni^{2+} was slightly higher than that of Zn^{2+}. All of these divalent metal ions showed steep Hill slopes (> 2.5) (Table 3), which we interpret to mean that divalent metal ions can act as their own PAMs at GPR39. The concentrations at which Zn^{2+} was active in this assay, *i.e.,* in the high micromolar range, were comparable to those seen *in vivo* (Foster *et al.*, 1993; Caroli *et al.*, 1994; Lu *et al.*, 2012). Zinc has been estimated at 200-320 uM in vivo in hippocampus mossy fibers (GPR39 is enriched in hippocampus (Fredrickson et al., 1983) and at levels >100 uM during synaptic transmission (Assaf and Chung, 1984). The concentrations we used in our experiments (3.4-340 μM) are in this range. Taken together, these results lead to the conclusion that GPR39-C3, LY2784544, GSK2636771, Zn^{2+} and Ni^{2+} can all act as agonists of GPR39-mediated Gq signaling, and that additionally, Zn^{2+} is a PAM of the responses of GPR39-C3, LY2784544 and GSK2636771.

Molecular Pharmacology Fast Forward. Published on October 17, 2016 as DOI: 10.1124/mol.116.106112
This article has not been copyedited and formatted. The final version may differ from this version.

Allosteric modulation of GPR39 Gs-mediated signaling

In addition, we measured GPR39-mediated Gs pathway signaling (*i.e.,* cAMP production) as described (see Methods). All three tested compounds, *i.e.,* GPR39-C3, LY2784544 and GSK2636771, showed Zn^{2+}-dependent Gs signaling (Fig. 5A-C; Table 4). Importantly, even GPR39-C3 showed a dramatic Zn^{2+}-dependency of this response, despite not doing so in either β-arrestin recruitment (Fig. 3A) or Gq signaling (Fig. 4A). In untransfected cells, or in the absence of Zn^{2+}, neither of the compounds showed GPR39-mediated Gs pathway signaling (Fig. 5D-F). At high concentrations, *i.e.,* 30 μM and higher, Zn^{2+} and Ni^{2+} also acted as weak partial agonists of GPR39-mediated Gs pathway signaling (Fig. 5G-I; Table 5). Thus, GPR39-C3, LY2784544, GSK2636771, Zn^{2+} and Ni^{2+} can all act as agonists of GPR39-mediated Gs signaling, and additionally, Zn^{2+} is a PAM for the Gs-mediated responses of GPR39-C3, LY2784544 and GSK2636771.

Effects of mutation of N-terminal histidine residues on GPR39-mediated signaling

A previous study showed that mutation of two N-terminal histidine residues to alanine (H17A/H19A) in GPR39 led to a dysfunction in GPR39-mediated Gq signaling (Storjohann *et al.*, 2008) such that Zn^{2+}-stimulated signaling was completely abolished. We wished to study the effects of these mutations further, both with respect to various signaling pathways, and to various agonists and PAMs. First, we established by cell-ELISA that the H17A/H19A double mutant of GPR39 was expressed similarly to the wildtype GPR39, both in the TANGO constructs as well as the “de-TANGO-ized” constructs (Supplementary Fig. 4). In Fig. 6 and Table 6, it can be seen that the

Molecular Pharmacology Fast Forward. Published on October 17, 2016 as DOI: 10.1124/mol.116.106112
This article has not been copyedited and formatted. The final version may differ from this version.

H17A/H19A double mutant of GPR39 had little effect on β-arrestin recruitment activity, both in response to the three small molecule compounds of interest, as well as the activity of Zn^{2+} as a PAM of these responses. The double mutation completely abolished Gq signaling stimulated by either Zn^{2+} or Ni^{2+} (Fig. 7D-F), consistent with the report of Storjohann *et al.* (2008). The double mutation had little or no effect on Gq signaling stimulated by GPR39-C3, LY2784544, or GSK2636771, both in the presence or in the absence of 100 μM Zn^{2+} (Fig. 7A-C; Table 7). As with Gq signaling, the double mutation completely abolished Gs signaling stimulated by either Zn^{2+} or Ni^{2+} (Fig. 8D-F). However, the double mutant showed reduced Gs signaling stimulated by GPR39-C3, LY2784544, or GSK2636771, with respect to both potency and efficacy (Fig. 8A-C; Table 8).

Molecular Pharmacology Fast Forward. Published on October 17, 2016 as DOI: 10.1124/mol.116.106112
This article has not been copyedited and formatted. The final version may differ from this version.

DISCUSSION

Here we report the discovery of novel GPR39 agonist scaffolds and the identification of zinc as a GPR39 PAM. These results for the first time identify zinc as a potent and frequently pathway- and probe-specific allosteric modulator for small-molecule GPR39 agonists. To discover these GPR39 agonists, we used a β-arrestin recruitment assay to screen several compound libraries comprising more than 5000 unique compounds for agonist activity at the orphan GPCR GPR39, which had previously been reported to be a divalent metal ion zinc receptor. Two compounds were found that had selective activity at GPR39 – the JAK2 inhibitor LY2784544 and the PI3K-β inhibitor GSK2636771 (Fig. 1 and 2). In additional studies, we showed that Zn^{2+} is an allosteric modulator of the responses of GPR39 to LY2784544 and GSK2636771, and that the allosteric actions of Zn^{2+} on these responses were stronger than for the selective GPR39 agonist, GPR39-C3 (Fig. 3). Currently, LY2784544 is being evaluated in patients with myeloproliferative neoplasm in two Phase I trials to investigate dose and schedule (I3X-MC-JHTA, NCT01134120; and I3X-MC-JHTC, NCT01520220), and a Phase II study to investigate efficacy (I3X-MC-JHTB, NCT01594723) (Ma *et al.*, 2013). Additionally, GSK2636771 is being tested in a Phase I/II trial in patients with PTEN-deficient advanced solid tumors (NCT01458067) (Thorpe *et al.*, 2014). Indeed when the potencies for activating GPR39 in the presence of Zn^{2+} were calculated, we found their EC_{50} values were in the sub- to single-digit nM range in whole cell assays. By comparison, the potency of LY2784544 in whole cell assays for inhibition of JAK2 proliferation was 20 nM (Ma et al, 2013) while GSK2636771 had a potency in whole cell

Molecular Pharmacology Fast Forward. Published on October 17, 2016 as DOI: 10.1124/mol.116.106112
This article has not been copyedited and formatted. The final version may differ from this version.

assays of 7-114 nM (Qu *et al.,* 2015). These results indicate that, in terms of the cellular context, the activities at GPR39 could predominate.

Given that these compounds are being tested in clinical trials, it should be of interest to establish whether they activate off-targets. Also, if side effects of these compounds are found, it may be possible to link the side effects to the off-targets rather than the targets, and thus possibly to provide clues as to the physiological function(s) of orphan off-targets. In a clinical study of LY2784544, diarrhea, nausea, anemia, and transient increases in serum creatinine, uric acid, and potassium have been reported, and attributed to a "typical tumor lysis syndrome" (Tefferi, 2012); however, it seems conceivable that at least some of these effects might be due to activation of GPR39. Interestingly, GPR39 is highly expressed in human colorectal adenocarcinoma HT-29 cells, and Zn^{2+} and a GPR39 agonist stimulated Gq signaling and promoted survival in these cells (Cohen, Azriel-Tamir, *et al.*, 2012; Boehm *et al.*, 2013; Cohen *et al.*, 2014). We have shown that GPR39-C3, LY2784544 and GSK2636771 strongly activate the Gq pathway in HT-29 cells by using the FLIPR assay (Supplementary Fig. 5). Since LY2784544 shows modulator activity in the presence of physiological concentrations of Zn^{2+}, it will be important to determine in clinical trials whether its side effects are due to its activity at GPR39.

Moreover, Zn^{2+} induced increased cell growth and survival in GPR39-expressing human prostate cancer PC3 cells (Dubi *et al.*, 2008; Asraf *et al.*, 2014). Importantly, prostate tissue is rich in Zn^{2+} (Györkey *et al.*, 1967; Zaichick VYe *et al.*, 1997). In the absence of

Molecular Pharmacology Fast Forward. Published on October 17, 2016 as DOI: 10.1124/mol.116.106112
This article has not been copyedited and formatted. The final version may differ from this version.

Zn^{2+}, the selective PI3Kβ inhibitor GSK2636771 significantly decreases cell viability in p110 β -reliant PTEN-deficient PC3 cells (Weigelt *et al.*, 2013). In the present study, we discovered that GSK2636771 could promote GPR39-selective intracellular signaling, which was markedly enhanced by the divalent metal ion Zn^{2+} (Figs. 3-5). Additionally, we have confirmed GPR39- and Gq-mediated Ca^{2+} release in PC3 cells after stimulation with GPR39 agonists in the presence of Zn^{2+} (Supplementary Fig. 6). Since GSK2636771 has been developed as a potential treatment for PTEN-deficient advanced solid tumors, including colorectal cancer, it may be important to consider possible off-target effects of this compound due to its actions at GPR39. In addition, and more generally, our approach shows that new activities for compounds, and new modulators for poorly-annotated GPCRs, can be discovered by screening of modestly-sized libraries of already-known small molecules.

The divalent metal ion Zn^{2+} has been reported to allosterically modulate GPCR function, not only GPR39 but also 5HT1A-serotonin (Barrondo and Sallés, 2009; Satała *et al.*, 2015), alpha (1A)-adrenoreceptor (Ciolek *et al.*, 2011), β2-adrenergic receptor (Swaminath *et al.*, 2002). Furthermore, the divalent metal ion Zn^{2+} can stimulate GPR68 (Abe-Ohya *et al.*, 2015) and GPRC6A (Pi and Quarles, 2012; Pi *et al.*, 2012) in the μM to mM range. Interestingly, Zn^{2+} modulates GPR39 activity *via* the Gq, Gs and β–arrestin pathways (Holst *et al.*, 2007). Other divalent cations, including Ni^{2+} (Holst *et al.*, 2007) and even Cr^{2+}, Fe^{2+} and Cd^{2+} (Huang *et al.,* 2015) can also activate GPR39. In general, most GPCRs can modulate one G-protein signaling pathway in addition to the β–arrestin pathway, although there are many exceptions. Our data show that

Molecular Pharmacology Fast Forward. Published on October 17, 2016 as DOI: 10.1124/mol.116.106112
This article has not been copyedited and formatted. The final version may differ from this version.

LY2784544 and GSK2636771 can stimulate Gq (Fig. 4), Gs (Fig. 5), and β–arrestin (Fig. 3) pathways strongly. However, the mechanisms of stimulation of these compounds may not be the same and may not be shared with Zn^{2+} or GPR39-C3. For example, the Zn^{2+} -dependent enhancement of potency in the Gq and β–arrestin pathways induced by LY2784544 and GSK2636771, which have similar structures, is much greater than that induced by GPR39-C3. (Fig. 3 and 4), though clearly additional studies are needed to clarify the molecular details responsible for these intriguing signaling differences.

The potency and efficacy of Zn^{2+} alone in the β–arrestin pathway are quite small (Fig. 3). In the TANGO assay, which requires overnight incubation with ligand, the toxicity of high concentrations of Zn^{2+} prevented measurement of β–arrestin recruitment at these concentrations. However, it has been shown that Ni^{2+} can stimulate β–arrestin recruitment to GPR39 using a BRET assay (Holst *et al.,* 2007), and presumably this would be similar with Zn^{2+}. In comparison with the activities of GPR39-C3, LY2784544 and GSK2636771, our results show that the responses to Zn^{2+} alone are quite small. We conclude that Zn^{2+} is acting as a small molecule PAM agonist at GPR39 for these two pathways.

Stimulation of the Gs (cAMP) pathway by compounds acting at GPR39 followed a very different pattern when compared with the Gq and β–arrestin pathways. The divalent

Molecular Pharmacology Fast Forward. Published on October 17, 2016 as DOI: 10.1124/mol.116.106112
This article has not been copyedited and formatted. The final version may differ from this version.

cations Zn^{2+} and Ni^{2+} stimulated this pathway on their own; additionally, the GPR39-C3 compound, even without Zn^{2+}, showed significant Gs activity (Fig. 5). This is in agreement with a previous study (Peukert *et al.*, 2014), which showed an EC_{50} value of 60 nM and an efficacy of 64% of the activity shown by 25 µM forskolin. Another study found that the GPR39 agonists AZ7914, AZ4237 and AZ1395 also stimulated cAMP responses without Zn^{2+} (Fjellström et al., 2015); however the phosphodiesterase inhibitor IBMX was used in that study, which makes estimation of the "true" pharmacological parameters of these compounds difficult. Our results showed that all three compounds, *i.e.,* GPR39-C3, LY2784544 and GSK2636771, had similar and significant Zn^{2+}-dependency in their Gs responses, and were thus acting as PAM agonists with respect to Zn^{2+} in the Gs pathway.

The differences in the activities of the divalent cations and GPR39-C3, LY2784544 and GSK2636771 at GPR39 suggest that there may be multiple binding sites or modes for divalent cations in GPR39. It has already been shown that two histidine residues in the N-terminus (H17 and H19) are involved in Zn^{2+} activity, since the Gq pathway response to concentrations of Zn^{2+} less than 1 mM is completely abolished by alanine substitution of these residues (Storjohann *et al.*, 2008b). Our results confirm these observations, and the response to Ni^{2+} was also abolished by these mutations (Fig. 7). Additionally, the Gs (cAMP) response to Zn^{2+} was also abolished by these mutations (Fig. 8). Thus, we conclude that H17 and H19 form one binding site for Zn^{2+} in GPR39. However, the H17A/H19A double mutation did not affect the activity of zinc, or the zinc-dependency of

Molecular Pharmacology Fast Forward. Published on October 17, 2016 as DOI: 10.1124/mol.116.106112
This article has not been copyedited and formatted. The final version may differ from this version.

the activities of GPR39-C3, LY2784544 and GSK2636771 in the Gq or β–arrestin recruitment assays (Fig. 6 and 7). From this, we conclude that there must be an additional zinc-binding site in GPR39, that the zinc-binding sites act independently of each other, and that the H17/H19 zinc-binding site is orthosteric, whereas the yet unknown additional site is allosteric.

In conclusion, here we report that the previously described 'selective' kinase inhibitors LY2784544 and GSK2636771 have unexpectedly selective PAM agonist activity with respect to Zn^{2+} at GPR39. All tested compounds induced Gq, Gs and β–arrestin signaling, and those responses are modulated by the divalent metal ion Zn^{2+} acting as a PAM agonist. We also clarified the roles of key residues in GPR39 relating only to divalent metal ion agonist activity by using mutagenesis. Although several ligands for GPR39 have been reported, whether there are endogenous ligands other than divalent metal ions for GPR39 is still not clear. Additionally, the physiological functions of GPR39 signaling *in vivo* remain to be determined and the scaffolds described here may provide starting points for novel chemical probes for GPR39.

Molecular Pharmacology Fast Forward. Published on October 17, 2016 as DOI: 10.1124/mol.116.106112
This article has not been copyedited and formatted. The final version may differ from this version.

Authorship Contributions:

Participated in research design: Sato, Huang, Kroeze, Roth

Conducted experiments: Sato, Huang, Kroeze

Performed data analysis: Sato, Huang, Kroeze

Wrote or contributed to the writing of the manuscript: Sato, Kroeze, Roth

Molecular Pharmacology Fast Forward. Published on October 17, 2016 as DOI: 10.1124/mol.116.106112
This article has not been copyedited and formatted. The final version may differ from this version.

References

Abe-Ohya R, Ishikawa T, Shiozawa H, Suda K, and Nara F (2015) Identification of metals from osteoblastic ST-2 cell supernatants as novel OGR1 agonists. *J Recept Signal Transduct* **35**:485–492.

Asraf H, Salomon S, Nevo A, Sekler I, Mayer D, and Hershfinkel M (2014) The ZnR/GPR39 interacts with the CaSR to enhance signaling in prostate and salivary epithelia. *J Cell Physiol* **229**:868–877.

Assaf, SY and Chung, S-H (1984) Release of endogenous Zn^{2+} from brain tissue during activity. *Nature* **308:** 734-736.

Barnea G, Strapps W, Herrada G, Berman Y, Ong J, Kloss B, Axel R, and Lee KJ (2008) The genetic design of signaling cascades to record receptor activation. *Proc Natl Acad Sci U S A* **105**:64–9.

Barrondo S, and Sallés J (2009) Allosteric modulation of 5-HT1A receptors by zinc: Binding studies. *Neuropharmacology* **56**:455–462.

Bhattacharyya S, Luan J, Farooqi IS, Keogh J, Montague C, Brennand J, Jorde L, Wareham NJ, and O'Rahilly S (2004) Studies of the neuromedin U-2 receptor gene in human obesity: evidence for the existence of two ancestral forms of the receptor. *J Endocrinol* **183**:115–20.

Bjarnadóttir TK, Gloriam DE, Hellstrand SH, Kristiansson H, Fredriksson R, and Schiöth HB (2006) Comprehensive repertoire and phylogenetic analysis of the G protein-coupled receptors in human and mouse. *Genomics* **88**:263–273.

Boehm M, Hepworth D, Loria PM, Norquay LD, Filipski KJ, Chin JE, Cameron KO, Brenner M, Bonnette P, Cabral S, Conn E, Ebner DC, Gautreau D, Hadcock J, Lee ECY, Mathiowetz AM, Morin M, Rogers L, Smith A, Vanvolkenburg M, and Carpino PA. (2013) Chemical probe identification platform for orphan GPCRs using focused compound screening: GPR39 as a case example. *ACS Med Chem Lett* **4**:1079–1084.

Caroli S, Alimonti A, Coni E, Petrucci F, Senofonte O, and Violante N (1994) The Assessment of Reference Values for Elements in Human Biological Tissues and Fluids: A Systematic Review. *Crit Rev Anal Chem* **24**:363–398.

Ciolek J, Maïga A, Marcon E, Servent D, and Gilles N (2011) Pharmacological characterization of zinc and copper interaction with the human alpha(1A)-adrenoceptor. *Eur J Pharmacol* **655**:1–8.

Cohen L, Azriel-Tamir H, Arotsker N, Sekler I, and Hershfinkel M (2012) Zinc sensing receptor signaling, mediated by GPR39, reduces butyrate-induced cell death in HT29 colonocytes via upregulation of clusterin. *PLoS One* **7**:1–13.

Cohen L, Sekler I, and Hershfinkel M (2014) The zinc sensing receptor, ZnR/GPR39, controls proliferation and differentiation of colonocytes and thereby tight junction formation in the colon. *Cell Death Dis* **5**:e1307.

Dubi N, Gheber L, Fishman D, Sekler I, and Hershfinkel M (2008) Extracellular zinc and zinc-citrate, acting through a putative zinc-sensing receptor, regulate growth and survival of prostate cancer cells. *Carcinogenesis* **29**:1692–1700.

Feighner SD, Tan CP, McKee KK, Palyha OC, Hreniuk DL, Pong SS, Austin CP, Figueroa D, MacNeil D, Cascieri M a, Nargund R, Bakshi R, Abramovitz M, Stocco R, Kargman S, O'Neill G, Van Der Ploeg LH, Evans J, Patchett AA, Smith RG, and Howard AD (1999) Receptor for motilin identified in the human gastrointestinal system. *Science* **284**:2184–2188.

Fjellström O, Larsson N, Yasuda S, Tsuchida T, Oguma T, Marley A, Wennberg-Huldt C, Hovdal D, Fukuda H, Yoneyama Y, Sasaki K, Johansson A, Lundqvist S, Brengdahl J, Isaacs RJ, Brown D, Geschwindner S, Benthem L, Priest C, and Turnbull A (2015) Novel Zn2+ Modulated GPR39 Receptor Agonists Do Not Drive Acute Insulin Secretion in Rodents. *PLoS One* **10**:e0145849.

Foster M, Leapman R, Li M, and Atwater I (1993) Elemental composition of secretory granules in pancreatic islets of Langerhans. *Biophys J* **64**:525–532.

Frederickson CJ, Klitenick MA, Manton WI, and Kirkpatrick JB (1983) Cytoarchitectonic distribution of zinc in the hippocampus of man and the rat. *Brain Research* **273:** 335-339.

Fredriksson R, and Schiöth HB (2005) The Repertoire of G-Protein – Coupled Receptors in Fully Sequenced Genomes. *Mol Pharmacol* **67:** 1414–1425.

Györkey F, Min KW, Huff JA, and Györkey P (1967) Zinc and magnesium in human prostate gland: normal, hyperplastic, and neoplastic. *Cancer Res* **27**:1348–53.

Holst B, Egerod KL, Jin C, Petersen PS, Østergaard MV, Hald J, Sprinkel AME, Størling J, Mandrup-Poulsen T, Holst JJ, Thams P, Orskov C, Wierup N, Sundler F, Madsen OD, and Schwartz TW (2009) G protein-coupled receptor 39 deficiency is associated with pancreatic islet dysfunction. *Endocrinology* **150**:2577–85.

Holst B, Egerod KL, Schild E, Vickers SP, Cheetham S, Gerlach L-O, Storjohann L, Stidsen CE, Jones R, Beck-Sickinger AG, and Schwartz TW (2007) GPR39 signaling is stimulated by zinc ions but not by obestatin. *Endocrinology* **148**:13–20.

Huang X-P, Karpiak J, Kroeze WK, Zhu H, Chen X, Moy SS, Saddoris KA, Nikolova VD, Farrell MS, Wang S, Mangano TJ, Deshpande DA, Jiang A, Penn RB, Jin J, Koller BH, Kenakin T, Shoichet BK, and Roth BL (2015) Allosteric ligands for the pharmacologically dark receptors GPR68 and GPR65. *Nature* **527:** 477-483.

Kenakin TP (2012) Biased signalling and allosteric machines: new vistas and challenges for drug discovery. *Br J Pharmacol* **165**:1659–69.

Kojima M, Haruno R, Nakazato M, Date Y, Murakami N, Hanada R, Matsuo H, and Kangawa K (2000) Purification and identification of neuromedin U as an endogenous ligand for an orphan receptor GPR66 (FM3). *Biochem Biophys Res Commun* **276**:435–8.

Kojima M, Hosoda H, Date Y, Nakazato M, Matsuo H, and Kangawa K (1999) Ghrelin is a growth-hormone-releasing acylated peptide from stomach. *Nature* **402**:656–60.

Komatsu H, Maruyama M, Yao S, Shinohara T, Sakuma K, Imaichi S, Chikatsu T, Kuniyeda K, Siu FK, Peng LS, Zhuo K, Mun LS, Han TM, Matsumoto Y, Hashimoto T, Miyajima N, Itoh Y, Ogi K, Habata Y, and Mori M (2014) Anatomical transcriptome of G protein-coupled receptors leads to the identification of a novel therapeutic candidate gpr52 for psychiatric disorders. *PLoS One* **9**:1–16.

Kroeze WK, Sassano MF, Huang X-P, Lansu K, McCorvy JD, Giguère PM, Sciaky N, and Roth BL (2015) PRESTO-Tango as an open-source resource for interrogation of the druggable human GPCRome. *Nat Struct Mol Biol* **22**:362–369.

Lauwers E, Landuyt B, Arckens L, Schoofs L, and Luyten W (2006) Obestatin does not activate orphan G protein-coupled receptor GPR39. *Biochem Biophys Res Commun* **351**:21–5.

Lu J, Stewart AJ, Sleep D, Sadler PJ, Pinheiro TJT, and Blindauer CA (2012) A molecular mechanism for modulating plasma Zn speciation by fatty acids. *J Am Chem Soc* **134**:1454–1457.

Ma L, Clayton JR, Walgren RA, Zhao B, Evans RJ, Smith MC, Heinz-Taheny KM, Kreklau EL, Bloem L, Pitou C, Shen W, Strelow JM, Halstead C, Rempala ME, Parthasarathy S, Gillig JR, Heinz LJ, Pei H, Wang Y, Stancato LF, Dowless MS, Iversen PW, and Burkholder TP (2013) Discovery and characterization of LY2784544, a small-molecule tyrosine kinase inhibitor of JAK2V617F. *Blood Cancer J* **3**:e109.

Molecular Pharmacology Fast Forward. Published on October 17, 2016 as DOI: 10.1124/mol.116.106112
This article has not been copyedited and formatted. The final version may differ from this version.

Manglik A, Lin H, Aryal DK, McCorvy JD, Dengler D, Corder G, Levit A, Kling RC, Bernat V, Hübner H, Huang X-P, Sassano MF, Giguère PM, Löber S, Duan D, Scherrer G, Kobilka BK, Gmeiner P, Roth BL, and Shoichet BK (2016) Structure-based discovery of opioid analgesics with reduced side effects. *Nature* **537:**185-190.

Młyniec K, Gaweł M, Librowski T, Reczyński W, Bystrowska B, and Holst B (2015) Investigation of the GPR39 zinc receptor following inhibition of monoaminergic neurotransmission and potentialization of glutamatergic neurotransmission. *Brain Res Bull* **115**:23–9.

Młyniec K, Gaweł M, and Nowak G (2015) Study of antidepressant drugs in GPR39 (zinc receptor^{-}/$^{-}$) knockout mice, showing no effect of conventional antidepressants, but effectiveness of NMDA antagonists. *Behav Brain Res* **287**:135–8.

Młyniec K, and Nowak G (2015) Up-regulation of the GPR39 Zn2+-sensing receptor and CREB/BDNF/TrkB pathway after chronic but not acute antidepressant treatment in the frontal cortex of zinc-deficient mice. *Pharmacol Rep* **67**:1135–40.

Młyniec K, Singewald N, Holst B, and Nowak G (2015) GPR39 Zn(2+)-sensing receptor: a new target in antidepressant development? *J Affect Disord* **174**:89–100.

Moran BM, Abdel-Wahab YH, Vasu S, Flatt PR, and McKillop AM (2015) GPR39 receptors and actions of trace metals on pancreatic beta cell function and glucose homoeostasis. *Acta Diabetol* **53**:279–293, Springer Milan.

Overington JP, Al-Lazikani B, and Hopkins AL (2006) How many drug targets are there? *Nat Rev Drug Discov* **5**:993–6.

Peukert S, Hughes R, Nunez J, He G, Yan Z, Jain R, Llamas L, Luchansky S, Carlson A, Liang G, Kunjathoor V, Pietropaolo M, Shapiro J, Castellana A, Wu X, and Bose A (2014) Discovery of 2-Pyridylpyrimidines as the First Orally Bioavailable GPR39 Agonists. *ACS Med Chem Lett* **5**:1114–8.

Pi M, and Quarles LD (2012) GPRC6A regulates prostate cancer progression. *Prostate* **72**:399–409.

Pi M, Wu Y, Lenchik NI, Gerling I, and Quarles LD (2012) GPRC6A Mediates the Effects of L-Arginine on Insulin Secretion in Mouse Pancreatic Islets. *Endocrinology* **153**:4608–15.

Popovics P, and Stewart AJ (2011) GPR39: a Zn(2+)-activated G protein-coupled receptor that regulates pancreatic, gastrointestinal and neuronal functions. *Cell Mol Life Sci* **68**:85–95.

Qu J, Rivero RA, Sanchez R, and Tedesco R (2015) Benzimidazole derivatives as PI3 kinase inhibitors. US Patent Application No. 14/712,991.

Rask-Andersen M, Masuram S, and Schiöth HB (2014) The Druggable Genome: Evaluation of Drug Targets in Clinical Trials Suggests Major Shifts in Molecular Class and Indication. *Annu Rev Pharmacol Toxicol* **54**:9–26.

Regard JB, Sato IT, and Coughlin SR (2008) Anatomical Profiling of G Protein-Coupled Receptor Expression. *Cell* **135**:561–571.

Roth BL, and Kroeze WK (2015) Integrated Approaches for Genome-wide Interrogation of the Druggable Non-olfactory G Protein-coupled Receptor Superfamily. J Biol Chem **290:**19471–7.

Satała G, Duszyńska B, Stachowicz K, Rafalo A, Pochwat B, Luckhart C, Albert PR, Daigle M, Tanaka KF, Hen R, Lenda T, Nowak G, Bojarski AJ, and Szewczyk B (2015) Concentration-Dependent Dual Mode of Zn Action at Serotonin 5-HT1A Receptors: In Vitro and In Vivo Studies. *Mol Neurobiol*, doi: 10.1007/s12035-015-9586-3.

Storjohann L, Holst B, and Schwartz TW (2008) Molecular mechanism of Zn2+ agonism in the extracellular domain of GPR39. *FEBS Lett* **582**:2583–2588.

Swaminath G, Steenhuis J, Kobilka B, Lee TAEW, and Hughes H (2002) Allosteric Modulation of β2 -Adrenergic Receptor by Zn2+. *Mol Pharmacol* **61**:65–72.

Tanaka K, Masu M, and Nakanishi S (1990) Structure and functional expression of the cloned rat neurotensin receptor. *Neuron* **4**:847–54.

Tefferi A (2012) JAK inhibitors for myeloproliferative neoplasms: clarifying facts from myths. *Blood* **119**:2721–2730.

Thorpe LM, Yuzugullu H, and Zhao JJ (2014) PI3K in cancer: divergent roles of isoforms, modes of activation and therapeutic targeting. *Nat Rev Cancer* **15**:7–24.

Vassilatis DK, Hohmann JG, Zeng H, Li F, Ranchalis JE, Mortrud MT, Brown A, Rodriguez SS, Weller JR, Wright AC, Bergmann JE, and Gaitanaris GA (2003) The G protein-coupled receptor repertoires of human and mouse. *Proc Natl Acad Sci U S A* **100**:4903–4908.

Verhulst PJ, Lintermans A, Janssen S, Loeckx D, Himmelreich U, Buyse J, Tack J, and Depoortere I (2011) GPR39, a receptor of the ghrelin receptor family, plays a role in the regulation of glucose homeostasis in a mouse model of early onset diet-induced obesity. *J Neuroendocrinol* **23**:490–500.

Vita N, Oury-Donat F, Chalon P, Guillemot M, Kaghad M, Bachy A, Thurneyssen O, Garcia S, Poinot-Chazel C, Casellas P, Keane P, Le Fur G, Maffrand JP, Soubrie P, Caput D, and Ferrara P (1998) Neurotensin is an antagonist of the human neurotensin NT2 receptor expressed in Chinese hamster ovary cells. *Eur J Pharmacol* **360**:265–72.

Weigelt B, Warne PH, Lambros MB, Reis-Filho JS, and Downward J (2013) PI3K pathway dependencies in endometrioid endometrial cancer cell lines. *Clin Cancer Res* **19**:3533–3544.

Yasuda S, Miyazaki T, Munechika K, Yamashita M, Ikeda Y, and Kamizono A (2007) Isolation of Zn2+ as an endogenous agonist of GPR39 from fetal bovine serum. *J Recept Signal Transduct Res* **27**:235–46.

Zaichick VYe, Sviridova TV, and Zaichick SV (1997) Zinc in the human prostate gland: normal, hyperplastic and cancerous. *Int Urol Nephrol* **29**:565–74.

Zeng F, Wind N, Mcclenaghan C, Verkuyl JM, Watson RP, and Nash MS (2012) GPR39 Is Coupled to TMEM16A in Intestinal Fibroblast-Like Cells. *PLoS One* **7**:1–11.

Zhang JV, Klein C, Ren PG, Kass S, VerDonck L, Moechars D, and Hsueh AJW (2007) Response to Comment on “Obestatin , a peptide encoded by the ghrelin gene, opposes ghrelin's effects on food intake". *Science* **315**:766.

Zhang JV, Ren PG, Avsian-Kretchmer O, Luo CW, Rauch R, Klein C, and Hsueh AJ. (2005) Obestatin, a Peptide Encoded by the Ghrelin Gene, Opposes Ghrelin’s Effects on Food Intake. *Science* **310**:996–999.

Molecular Pharmacology Fast Forward. Published on October 17, 2016 as DOI: 10.1124/mol.116.106112
This article has not been copyedited and formatted. The final version may differ from this version.

This work was supported by the National Institues of Health [Grant U01-MH104974].

Address reprint requests to: Bryan L. Roth, Genetic Medicine Building Rm 4072, 120 Mason Farm Rd, Chapel Hill, NC 27599

E-mail: bryan_roth@med.unc.edu

Molecular Pharmacology Fast Forward. Published on October 17, 2016 as DOI: 10.1124/mol.116.106112
This article has not been copyedited and formatted. The final version may differ from this version.

Figure Legends

Fig. 1. Summary of drug screening at GPR39 using the TANGO β-arrestin recruitment assay. (A) Screening was carried out in quadruplicate at 10 μM drug concentration. After excluding promiscuous activators, LY2784544 and GSK2636771 were identified as GPR39-selective agonist for the β–arrestin pathway (B and C). (B) Structures of LY2784544 (middle) and GSK2636771 (right) and a previously described GPR39 (left) agonist, GPR39-C3. (C) Activities of LY2784544 and GSK2636771 at GPR39 and 11 additional understudied GPCRs.

Fig. 2. GPCRome (PRESTO-Tango) analysis of three compounds GPR39-C3 (A), LY2784544 (B) and GSK2636771 (C), respectively. These assays were performed using 1 μM concentrations of each compound with 100 μM $ZnCl_2$. The results are the mean ± S.E.M. of quadruplicate determinations. PC (blue); Positive control, 1 μM quinpirole against DRD2.

Fig. 3. Concentration-dependent and GPR39-dependent β-arrestin recruitment as measured by the TANGO assay in response to GPR39-C3 (A), LY2784544 (B) or GSK2636771 (C) in the presence various concentrations of Zn^{2+}. (D) Zn^{2+} stimulations were carried out at several different incubation times with Zn^{2+} from 5 min to 6 hr, followed by washing and incubation with fresh medium or overnight incubation with Zn^{2+}. The results are expressed as the fold of basal, and are the mean ± S.E.M. of three independent experiments, each performed in quadruplicate.

Molecular Pharmacology Fast Forward. Published on October 17, 2016 as DOI: 10.1124/mol.116.106112
This article has not been copyedited and formatted. The final version may differ from this version.

Fig. 4. Concentration-dependent and GPR39-dependent PI hydrolysis (G_q pathway) in response to GPR39-C3 (A), LY2784544 (B) or GSK2636771 (C) with various concentrations of Zn^{2+}. According to allosteric operational model, the allosteric parameters were calculated (Kenakin, 2012). τ_A is the orthosteric agonist (LY2784544 and GSK2736771) efficacy parameter. Since allosteric modulators in this study showed agonist activity, the allosteric modulator efficacy τ_B is therefore greater than 0. Concentration-dependent and GPR39-dependent PI hydrolysis (G_q pathway) in response to $ZnCl_2$ (D), $NiCl_2$ (E) and $NiSO_4$ (F). Black dots show response to compounds in untransfected HEK293T cells. The results are the mean ± S.E.M. of at least three independent experiments performed in quadruplicate (compounds and $ZnCl_2$) or duplicate ($NiCl_2$).

Fig. 5. Concentration-dependent and GPR39-dependent cAMP (Gs) responses as measured by the Glosensor assay to GPR39-C3 (A), LY2784544 (B) or GSK2636771 (C) with various concentrations of Zn^{2+}. Responses in the absence of Zn^{2+} are shown in (D), (E) and (F). Responses to $ZnCl_2$, $NiCl_2$ and $NiSO_4$ are shown in (G) and (H) and (I), respectively. The results are the mean ± S.E.M. of at least three independent experiments performed in quadruplicate.

Fig. 6. Concentration-dependent β-arrestin recruitment responses of wild-type and H17A/H19A mutant receptors to GPR39-C3 (A), LY2784544 (B), and GSK2636771 (C) in the presence and absence of 100 μM Zn^{2+}as measured by the TANGO assay. The results are the mean ± S.E.M. of at least five independent experiments, each done in quadruplicate.

Molecular Pharmacology Fast Forward. Published on October 17, 2016 as DOI: 10.1124/mol.116.106112
This article has not been copyedited and formatted. The final version may differ from this version.

Fig. 7. Concentration-dependent PI hydrolysis responses (G_q pathway) to GPR39-C3 (A), LY2784544 (B), and GSK2636771 (C) in the presence and absence of 100 μM Zn^{2+}at wild-type and H17A/H19A mutant receptors. Concentration-dependent PI hydrolysis responses (G_q pathway) to $ZnCl_2$ (D), $NiCl_2$ (E) or $NiSO_4$ (F). The results are the mean ± S.E.M. of at least three independent experiments, each done in quadruplicate.

Fig. 8. Concentration-dependent cAMP production (Gs pathway) to GPR39-C3 (A), LY2784544 (B), and GSK2636771 (C) in the presence and absence of 100 μM Zn^{2+} at wild-type and H17A/H19A mutant receptors as measured by the Glosensor assay. Concentration-dependent cAMP production (Gs pathway) to $ZnCl_2$ (D), $NiCl_2$ (E) or NiSO4 (F) at wild-type or H17A/H19A mutant receptors as measured by the Glosensor assay. The results are the mean ± S.E.M. of at least eight independent experiments, each in quadruplicate.

Molecular Pharmacology Fast Forward. Published on October 17, 2016 as DOI: 10.1124/mol.116.106112
This article has not been copyedited and formatted. The final version may differ from this version.

Table 1. Pharmacological parameters of results shown in Fig. 3A-C. Top and Bottom are expressed as fold of basal and Log EC_{50} as logged EC_{50} [M].

		$ZnCl_2$											
		316 µM *N* = 3		**100 µM** *N* = 8		**31.6 µM** *N* = 3		**10 µM** *N* = 3		**3.2 µM** *N* = 3		**0 µM** *N* = 8	
GPR39-C3	Top	0.04	± 0.00	30.27	± 0.57	22.03	± 0.71	23.23	± 0.88	26.81	± 1.92	33.25	± 2.3
	Bottom	0.01	± 0.00	1.09	± 0.36	0.98	± 0.21	0.99	± 0.20	0.95	± 0.19	1.00	± 0.1
	Log EC_{50}	-8.63	± 0.17	-7.99	± 0.04	-7.09	± 0.06	-6.72	± 0.06	-6.40	± 0.11	-6.22	± 0.1
	Hill Slope	0.82	± 0.24	1.52	± 0.17	0.79	± 0.07	0.83	± 0.08	0.72	± 0.07	0.69	± 0.0
LY2784544	Top	0.03	± 0.00	23.16	± 0.52	11.38	± 0.45	7.99	± 0.33	6.59	± 0.51	7.10	± 0.7
	Bottom	0.01	± 0.00	0.89	± 0.25	1.02	± 0.12	0.97	± 0.06	0.92	± 0.05	1.00	± 0.0
	Log EC_{50}	-8.93	± 0.27	-8.17	± 0.04	-6.86	± 0.06	-6.26	± 0.04	-6.03	± 0.07	-5.81	± 0.1
	Hill Slope	1.10	± 0.66	1.45	± 0.15	1.28	± 0.17	1.61	± 0.20	1.51	± 0.25	1.27	± 0.1
GSK26367771	Top	0.03	± 0.00	22.56	± 0.59	22.96	± 3.48	10.84	± 0.99	>153.7	-	>73.15	-
	Bottom	0.00	± 0.00	0.83	± 0.21	1.05	± 0.16	0.99	± 0.04	0.97	± 0.05	1.00	± 0.0
	Log EC_{50}	-7.96	± 0.29	-7.07	± 0.04	-5.42	± 0.16	-5.31	± 0.07	>-4.07	-	>-4.25	-
	Hill Slope	0.64	± 0.25	1.18	± 0.11	1.04	± 0.17	1.66	± 0.21	1.50	± 1.02	1.59	± 0.8

Molecular Pharmacology Fast Forward. Published on October 17, 2016 as DOI: 10.1124/mol.116.106112
This article has not been copyedited and formatted. The final version may differ from this version.

Table 2. Pharmacological parameters of results shown in Figs. 3A, B and C. Top and Bottom are expressed as fold of basal and Log EC_{50} as logged EC_{50} [M].

		$ZnCl_2$			
		316 μM *N* = 4	**100 μM** *N* = 4	**31.6 μM** *N* = 4	**0 μM** *N* = 4
GPR39-C3	Top	2.59 ± 0.06	3.21 ± 0.08	2.87 ± 0.08	3.07 ± 0.10
	Bottom	1.40 ± 0.09	1.18 ± 0.11	0.96 ± 0.10	1.00 ± 0.10
	Log EC_{50}	-8.49 ± 0.13	-8.48 ± 0.10	-8.16 ± 0.11	-8.00 ± 0.12
	Hill Slope	1.29 ± 0.46	1.20 ± 0.30	1.18 ± 0.30	0.94 ± 0.23
LY2784544	Top	3.40 ± 0.38	3.94 ± 0.30	4.57 ± 0.12	4.41 ± 0.07
	Bottom	1.92 ± 0.07	1.31 ± 0.11	1.07 ± 0.22	1.00 ± 0.22
	Log EC_{50}	-9.36 ± 0.14	-8.51 ± 0.14	-6.98 ± 0.16	-6.35 ± 0.19
	Hill Slope	1.30 ± 0.18	0.63 ± 0.17	0.79 ± 0.15	0.94 ± 0.59
GSK2636771	Top	3.47 ± 0.09	3.68 ± 0.12	3.75 ± 0.27	3.68 ± 0.63
	Bottom	1.91 ± 0.15	1.36 ± 0.12	1.08 ± 0.08	1.01 ± 0.05
	Log EC_{50}	-8.60 ± 0.18	-7.97 ± 0.13	-6.67 ± 0.14	-5.99 ± 0.25
	Hill Slope	1.01 ± 0.38	0.86 ± 0.20	1.01 ± 0.25	1.01 ± 0.28

Molecular Pharmacology Fast Forward. Published on October 17, 2016 as DOI: 10.1124/mol.116.106112
This article has not been copyedited and formatted. The final version may differ from this version.

Table 3. Pharmacological parameters of results shown in Figs. 3D, E and F. Top and Bottom are expressed as fold of basal and Log EC_{50} as logged EC_{50} [M].

	$ZnCl_2$ *N* = 3	**$NiCl_2$** *N* = 3	**$NiSO_4$** *N* = 3
Top	2.19 ± 0.06	2.20 ± 0.08	2.58 ± 0.10
Bottom	1.00 ± 0.03	0.98 ± 0.04	1.00 ± 0.05
Log EC50	-4.09 ± 0.05	-4.73 ± 0.07	-4.88 ± 0.08
Hill Slope	3.23 ± 1.40	2.53 ± 0.67	3.46 ± 1.95

Molecular Pharmacology Fast Forward. Published on October 17, 2016 as DOI: 10.1124/mol.116.106112
This article has not been copyedited and formatted. The final version may differ from this version.

Table 4. Pharmacological parameters of the results shown in Figs. 4A, B and C. Top and Bottom are expressed as fold of basal and Log EC_{50} as logged EC_{50} [M]. N.D. - could not determine.

		$ZnCl_2$					
		316 μM *N = 3*	**100 μM** *N* = 13	**31.6 μM** *N* = 3	**10 μM** *N* = 3	**3.16 μM** *N* = 3	**0 μM** *N* = 13
GPR39-C3	Top	22.76 ± 0.89	7.68 ± 0.15	3.18 ± 0.13	N.D. -	N.D. -	N.D.
	Bottom	2.33 ± 0.24	1.38 ± 0.05	1.29 ± 0.04	N.D. -	N.D. -	N.D.
	Log EC_{50}	-7.05 ± 0.07	-6.72 ± 0.04	-6.17 ± 0.08	N.D. -	N.D. -	N.D.
	Hill Slope	0.87 ± 0.10	1.01 ± 0.08	1.70 ± 0.45	N.D. -	N.D. -	N.D.
LY2784544	Top	18.86 ± 0.38	7.24 ± 0.19	1.96 ± 0.07	N.D. -	N.D. -	N.D.
	Bottom	2.04 ± 0.21	1.20 ± 0.10	1.12 ± 0.03	N.D. -	N.D. -	N.D.
	Log EC_{50}	-7.75 ± 0.05	-7.37 ± 0.08	-6.47 ± 0.08	N.D. -	N.D. -	N.D.
	Hill Slope	1.14 ± 0.12	1.13 ± 0.37	3.31 ± 3.73	N.D. -	N.D. -	N.D.
GSK2636771	Top	16.41 ± 0.51	4.80 ± 0.12	N.D. -	N.D. -	N.D. -	N.D.
	Bottom	1.93 ± 0.18	1.10 ± 0.05	N.D. -	N.D. -	N.D. -	N.D.
	Log EC_{50}	-7.12 ± 0.06	-7.09 ± 0.05	N.D. -	N.D. -	N.D. -	N.D.
	Hill Slope	1.10 ± 0.14	1.29 ± 0.17	N.D. -	N.D. -	N.D. -	N.D.

Molecular Pharmacology Fast Forward. Published on October 17, 2016 as DOI: 10.1124/mol.116.106112
This article has not been copyedited and formatted. The final version may differ from this version.

Table 5. Pharmacological parameters of results shown in Figs. 4G, H and I. The results are the mean ± S.E.M. of five independent experiments performed in quadruplicate. Top and Bottom are expressed as fold of basal and Log EC_{50} as logged EC_{50} [M].

	$ZnCl_2$ *N* = 7	**$NiCl_2$** *N* = 5	**$NiSO_4$** *N* = 5
Top	4.22 ± 0.20	2.99 ± 0.07	3.24 ± 0.12
Bottom	0.95 ± 0.02	0.93 ± 0.02	0.92 ± 0.02
Log EC_{50}	-3.42 ± 0.04	-4.04 ± 0.04	-3.91 ± 0.06
Hill Slope	2.62 ± 0.57	1.75 ± 0.24	1.25 ± 0.16

Molecular Pharmacology Fast Forward. Published on October 17, 2016 as DOI: 10.1124/mol.116.106112
This article has not been copyedited and formatted. The final version may differ from this version.

Table 6. Pharmacological parameters of results shown in Fig. 6. Top and Bottom are expressed as fold of basal and Log EC_{50} as logged EC_{50} [M]. N.D. - could not determine.

		WT		H17A/H19A	
		$ZnCl_2$ (+) *N* = 8	**$ZnCl_2$ (-)** *N* = 8	**$ZnCl_2$ (+)** *N* = 5	**$ZnCl_2$ (-)** *N* = 5
GPR39-C3	Top	30.27 ± 0.57	33.25 ± 2.31	25.87 ± 0.55	29.07 ± 2.02
	Bottom	1.09 ± 0.36	1.00 ± 0.16	1.08 ± 0.34	1.00 ± 0.24
	Log EC_{50}	-7.99 ± 0.04	-6.22 ± 0.11	-7.76 ± 0.04	-6.43 ± 0.10
	Hill Slope	1.52 ± 0.17	0.69 ± 0.05	1.51 ± 0.18	0.84 ± 0.10
LY2784544	Top	23.16 ± 0.52	7.10 ± 0.78	19.26 ± 0.56	7.23 ± 0.97
	Bottom	0.89 ± 0.25	1.00 ± 0.03	0.91 ± 0.27	1.00 ± 0.06
	Log EC_{50}	-8.17 ± 0.04	-5.81 ± 0.11	-8.07 ± 0.04	-5.91 ± 0.12
	Hill Slope	1.45 ± 0.15	1.27 ± 0.16	1.61 ± 0.23	1.57 ± 0.38
GSK2636771	Top	22.61 ± 0.59	N.D. -	22.85 ± 0.93	N.D. -
	Bottom	0.831 ± 0.21	1.00 ± 0.03	0.91 ± 0.27	1.00 ± 0.07
	Log EC_{50}	-7.068 ± 0.04	> -4.00 -	-6.94 ± 0.06	> -4.00 -
	Hill Slope	1.179 ± 0.11	1.59 ± 0.86	1.05 ± 0.13	1.703 ± 0.75

Molecular Pharmacology Fast Forward. Published on October 17, 2016 as DOI: 10.1124/mol.116.106112
This article has not been copyedited and formatted. The final version may differ from this version.

Table 7. Pharmacological parameters of results shown in Fig. 7. Top and Bottom are expressed fold of basal and Log EC_{50} as logged EC_{50} [M].

		WT		H17A/H19A	
		$ZnCl_2$ (+) *N* = 4	**$ZnCl_2$ (-)** *N* = 4	**$ZnCl_2$ (+)** *N* = 3	**$ZnCl_2$ (-)** *N* = 3
GPR39-C3	Top	3.21 ± 0.08	3.07 ± 0.10	3.72 ± 0.14	3.75 ± 0.2
	Bottom	1.18 ± 0.11	1.00 ± 0.10	1.07 ± 0.17	1.03 ± 0.1
	Log EC_{50}	-8.48 ± 0.10	-8.00 ± 0.12	-8.30 ± 0.14	-7.17 ± 0.1
	Hill Slope	1.20 ± 0.30	0.94 ± 0.23	1.01 ± 0.29	0.90 ± 0.2
LY2784544	Top	3.94 ± 0.12	4.41 ± 0.38	3.77 ± 0.13	3.85 ± 0.1
	Bottom	1.31 ± 0.22	1.00 ± 0.07	1.09 ± 0.27	1.03 ± 0.0
	Log EC_{50}	-8.51 ± 0.16	-6.35 ± 0.14	-8.72 ± 0.18	-6.23 ± 0.0
	Hill Slope	0.63 ± 0.15	0.94 ± 0.18	0.88 ± 0.29	1.15 ± 0.1
GSK26367771	Top	3.68 ± 0.12	3.68 ± 0.63	3.74 ± 0.12	3.00 ± 0.1
	Bottom	1.36 ± 0.12	1.01 ± 0.05	1.14 ± 0.15	1.01 ± 0.0
	Log EC_{50}	-7.97 ± 0.13	-5.99 ± 0.25	-8.16 ± 0.13	-5.99 ± 0.0
	Hill Slope	0.86 ± 0.20	1.01 ± 0.28	0.95 ± 0.24	1.35 ± 0.1

Molecular Pharmacology Fast Forward. Published on October 17, 2016 as DOI: 10.1124/mol.116.106112
This article has not been copyedited and formatted. The final version may differ from this version.

Table 8. Pharmacological parameters of the results shown in Figs. 8A-C. The results are the mean ± S.E.M. of least eight independent experiments, each in quadruplicate. Top and Bottom are expressed as fold of basal and Log EC_{50} as logged EC_{50} [M]. The statistical significance of difference in values between wild type and mutant was determined using a one-sided *t* test (**p*<0.05). N.D. could not determine.

		WT		**H17A/H19A**	
		$ZnCl_2$ (+) *N* = 13	**$ZnCl_2$ (-)** *N* = 13	**$ZnCl_2$ (+)** *N* = 8	**$ZnCl_2$ (-)** *N* = 8
GPR39-C3	Top	7.68 ± 0.11	N.D. -	6.01 ± 0.13 *	N.D. -
	Bottom	1.38 ± 0.17	N.D. -	1.37 ± 0.18	N.D. -
	Log EC_{50}	-6.72 ± 0.10	N.D. -	-6.49 ± 0.12 *	N.D. -
	Hill Slope	1.01 ± 0.37	N.D. -	1.22 ± 0.22	N.D. -
LY2784544	Top	7.24 ± 0.20	N.D. -	4.86 ± 0.13 *	N.D. -
	Bottom	1.20 ± 0.06	N.D. -	1.17 ± 0.04	N.D. -
	Log EC_{50}	-7.37 ± 0.05	N.D. -	-7.08 ± 0.05 *	N.D. -
	Hill Slope	1.13 ± 0.12	N.D. -	1.35 ± 0.17	N.D. -
GSK26367771	Top	4.80 ± 0.12	N.D. -	3.84 ± 0.12 *	N.D. -
	Bottom	1.10 ± 0.05	N.D. -	1.06 ± 0.03	N.D. -
	Log EC_{50}	-7.09 ± 0.05	N.D. -	-6.46 ± 0.06 *	N.D. -
	Hill Slope	1.29 ± 0.17	N.D. -	1.20 ± 0.16	N.D. -

Molecular Pharmacology Fast Forward. Published on October 17, 2016 as DOI: 10.1124/mol.116.106112
This article has not been copyedited and formatted. The final version may differ from this version.

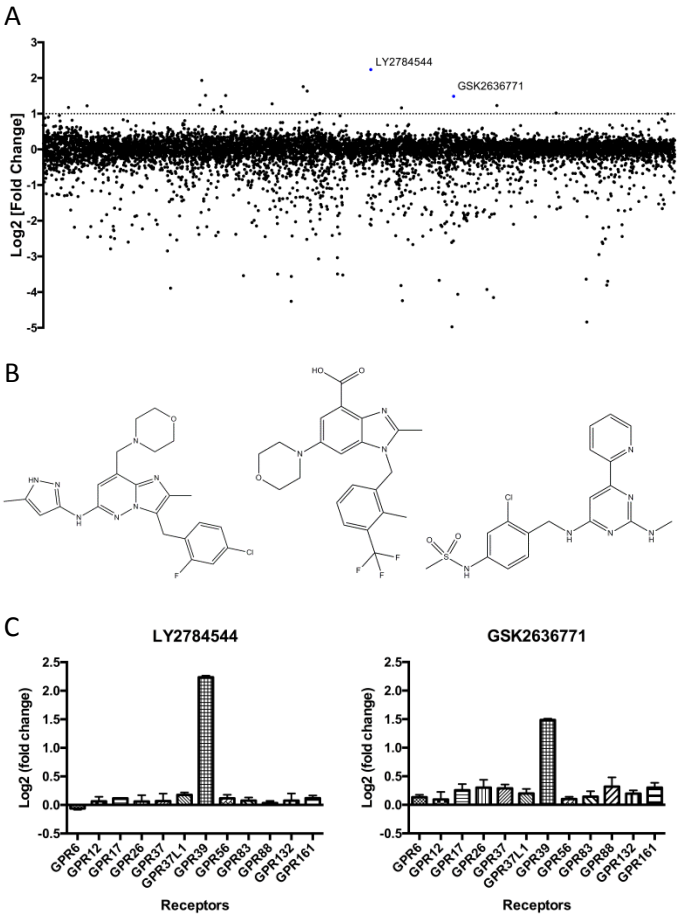

Figure 1

Molecular Pharmacology Fast Forward. Published on October 17, 2016 as DOI: 10.1124/mol.116.106112
This article has not been copyedited and formatted. The final version may differ from this version.

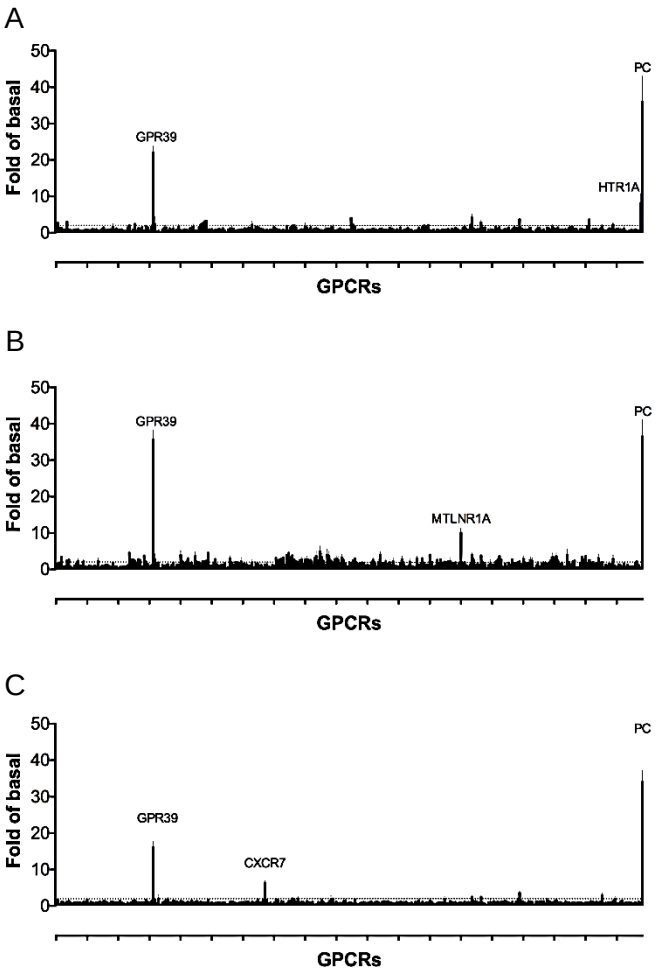

Figure 2

Molecular Pharmacology Fast Forward. Published on October 17, 2016 as DOI: 10.1124/mol.116.106112
This article has not been copyedited and formatted. The final version may differ from this version.

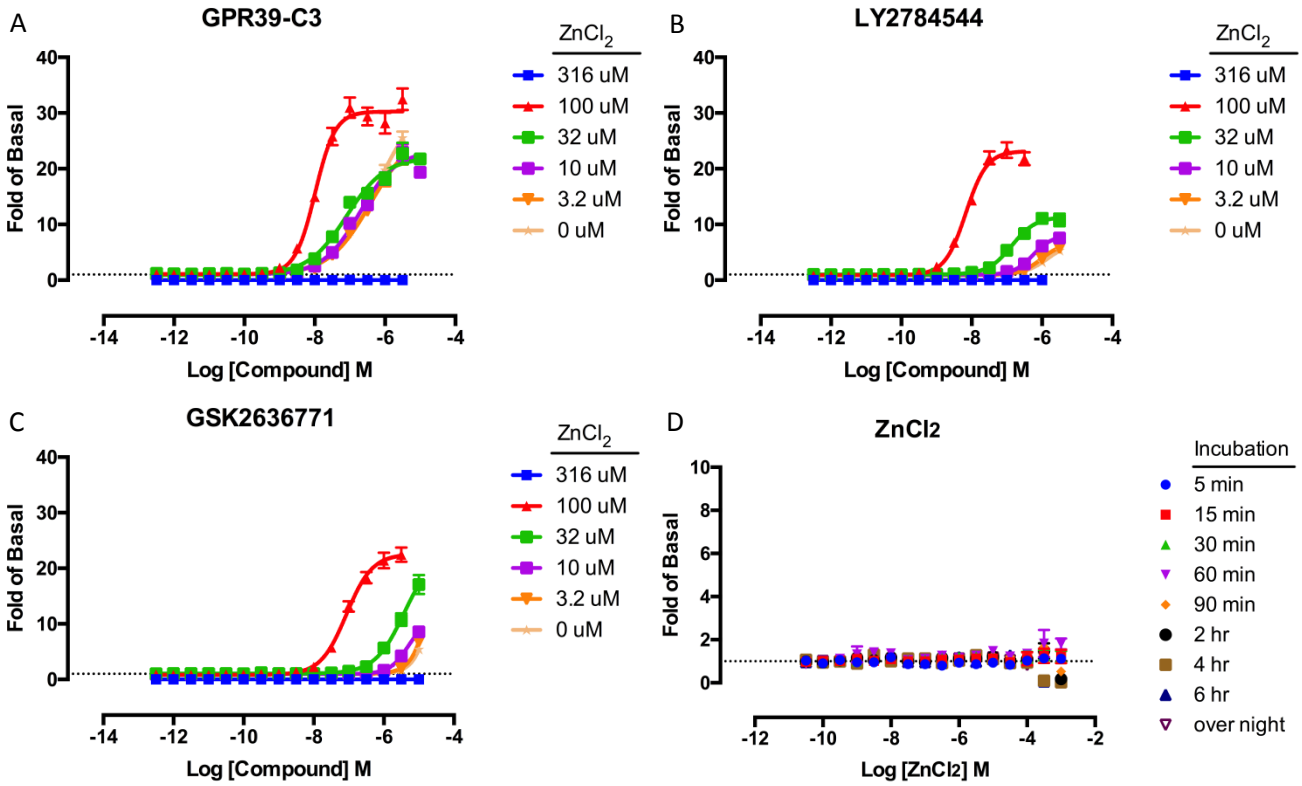

Figure 3

Molecular Pharmacology Fast Forward. Published on October 17, 2016 as DOI: 10.1124/mol.116.106112
This article has not been copyedited and formatted. The final version may differ from this version.

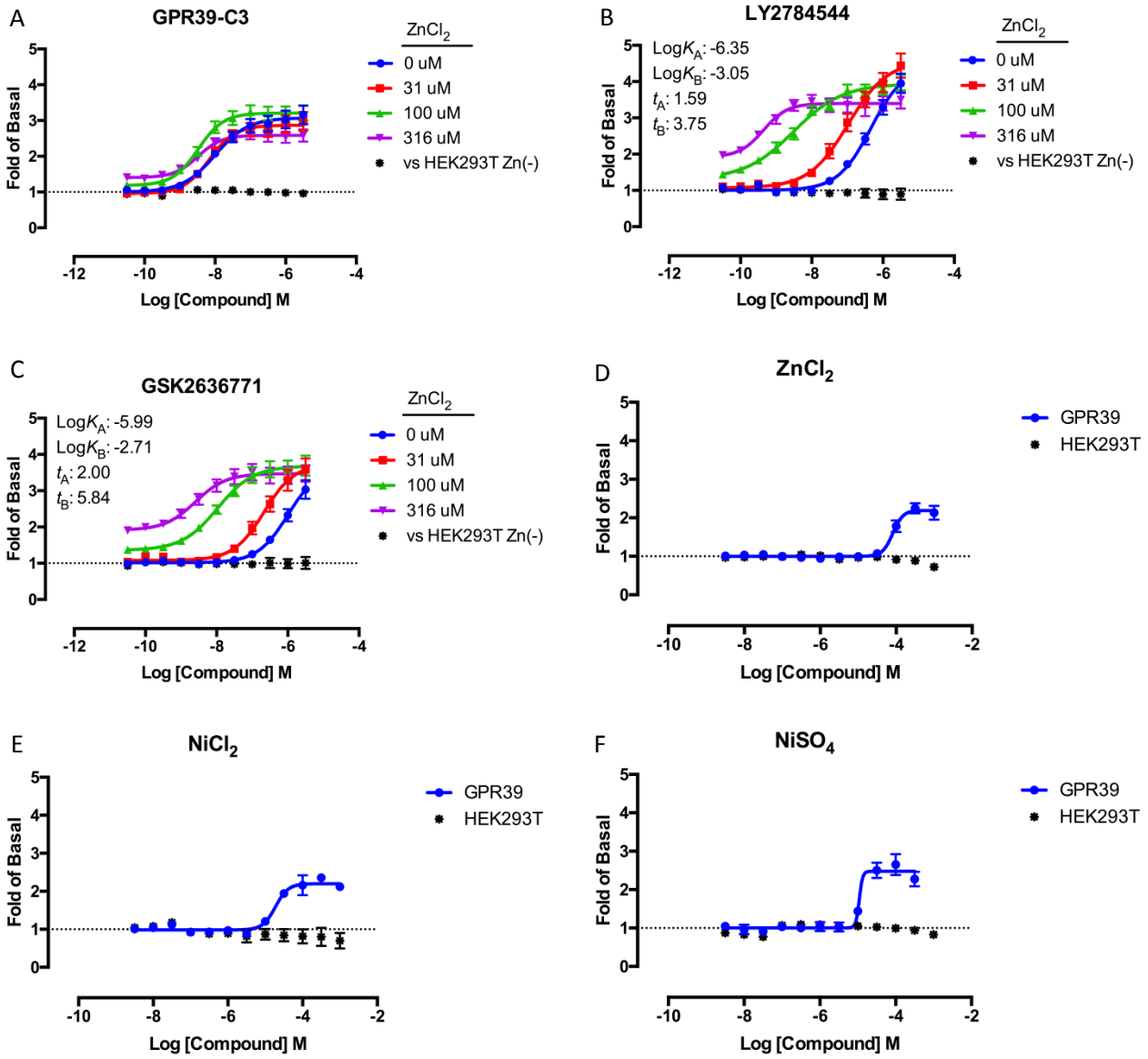

Figure 4

Molecular Pharmacology Fast Forward. Published on October 17, 2016 as DOI: 10.1124/mol.116.106112
This article has not been copyedited and formatted. The final version may differ from this version.

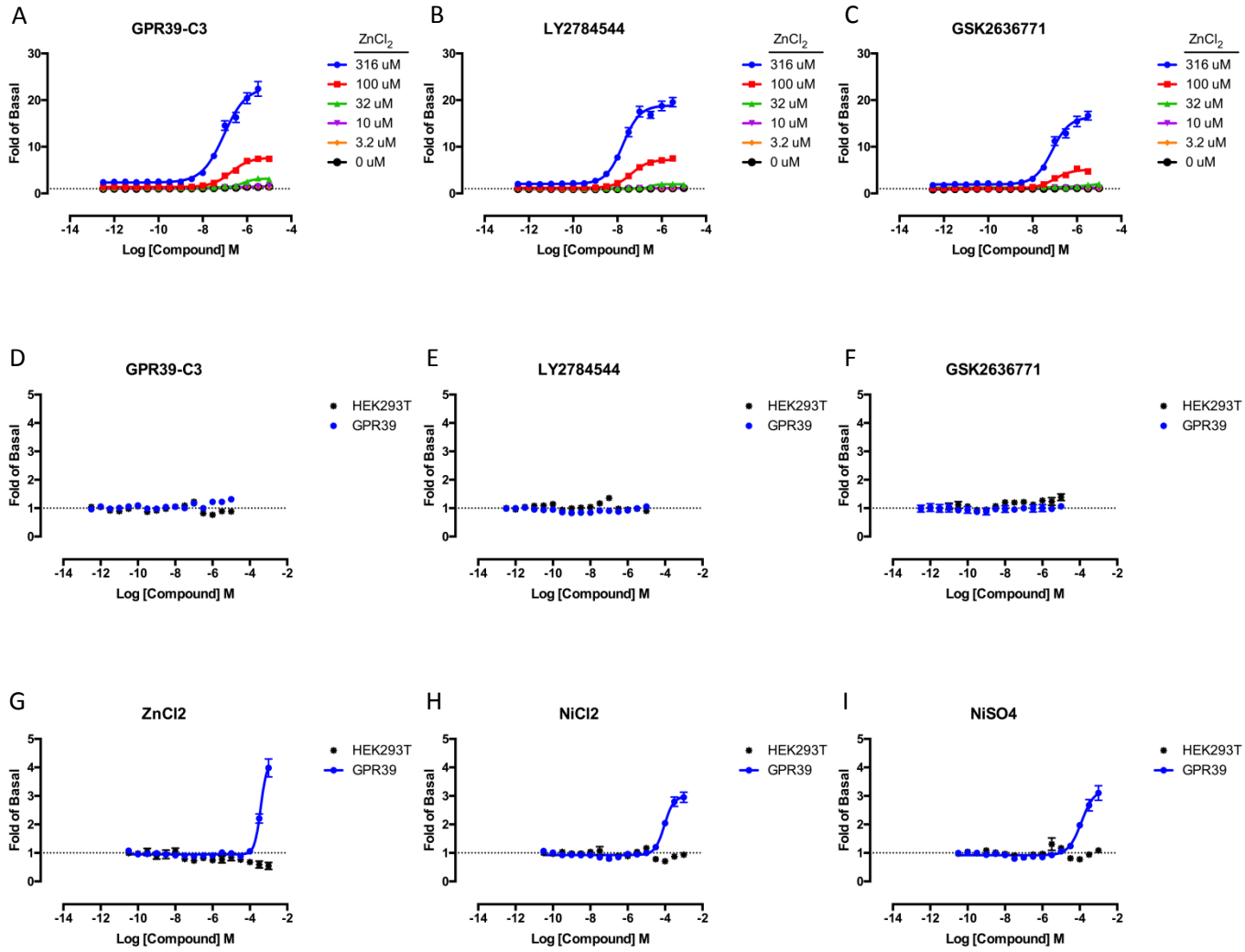

Figure 5

Molecular Pharmacology Fast Forward. Published on October 17, 2016 as DOI: 10.1124/mol.116.106112
This article has not been copyedited and formatted. The final version may differ from this version.

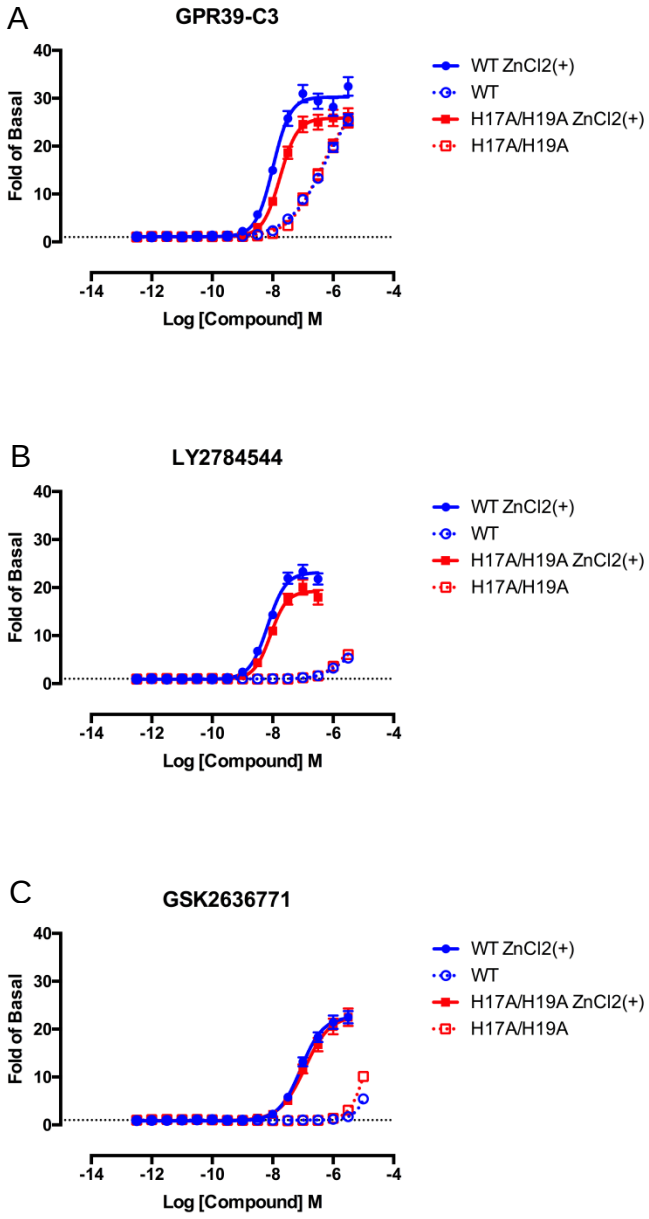

Figure 6

Molecular Pharmacology Fast Forward. Published on October 17, 2016 as DOI: 10.1124/mol.116.106112
This article has not been copyedited and formatted. The final version may differ from this version.

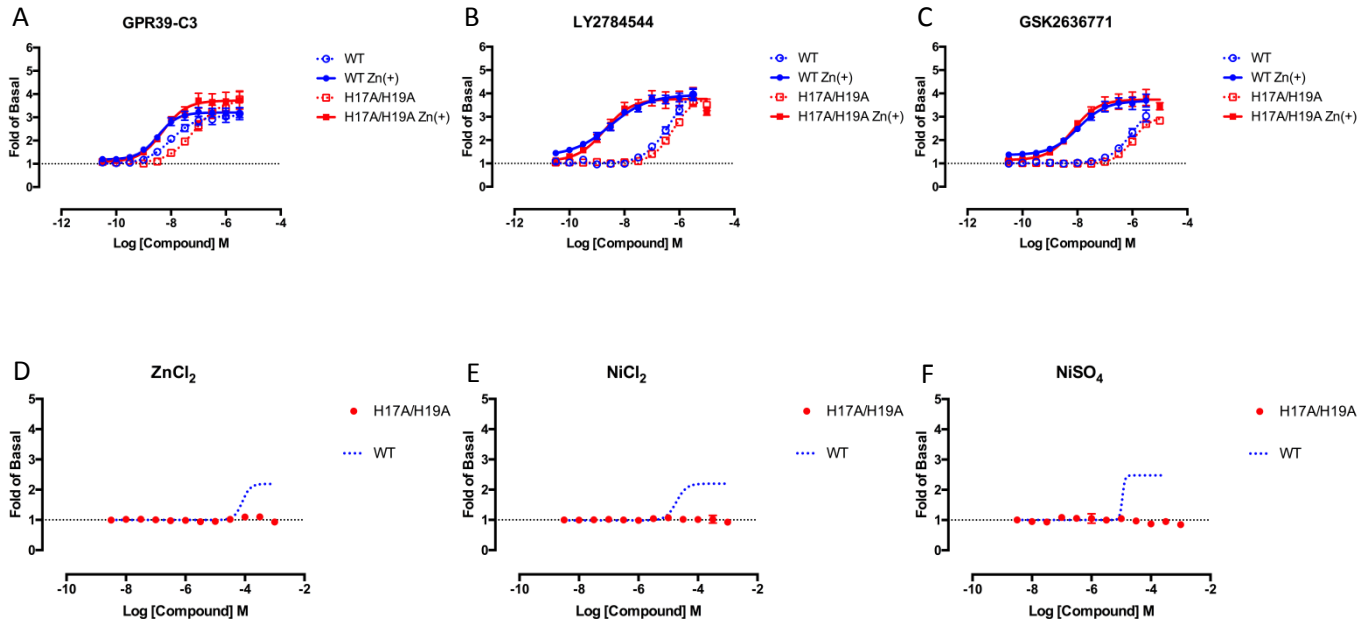

Figure 7

Molecular Pharmacology Fast Forward. Published on October 17, 2016 as DOI: 10.1124/mol.116.106112
This article has not been copyedited and formatted. The final version may differ from this version.

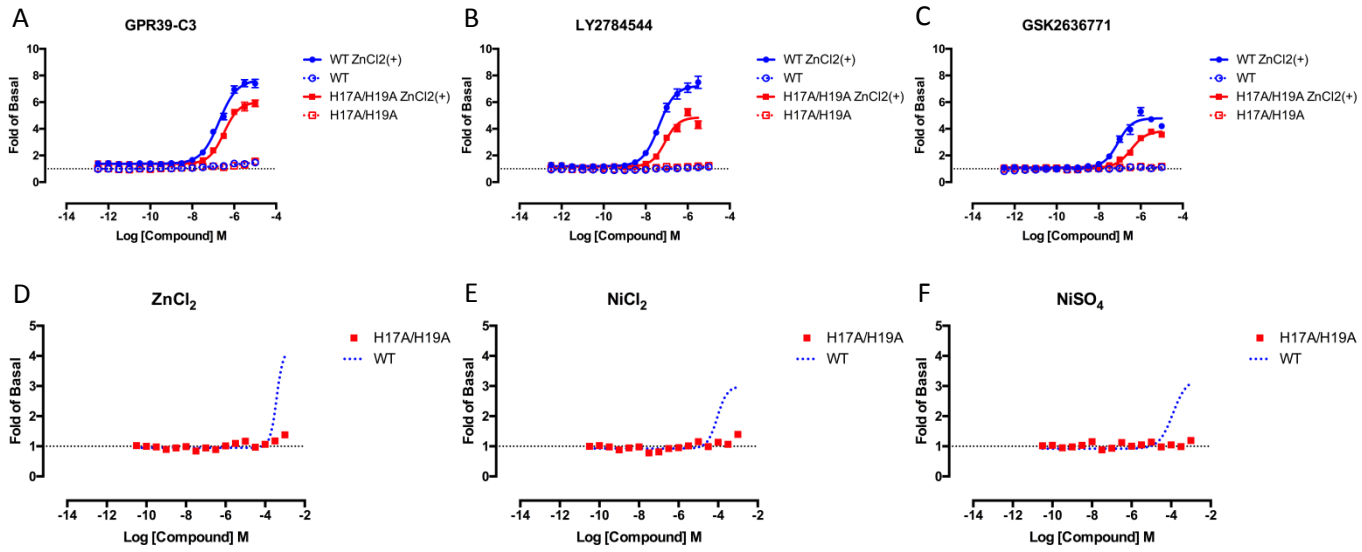

Figure 8

Discovery and characterization of novel GPR39 agonists allosterically modulated by zinc

Seiji Sato, Xi-Ping Huang, Wesley K. Kroeze and Bryan L. Roth

Molecular Pharmacology

Supplementary Information

Supplementary Figure 1.

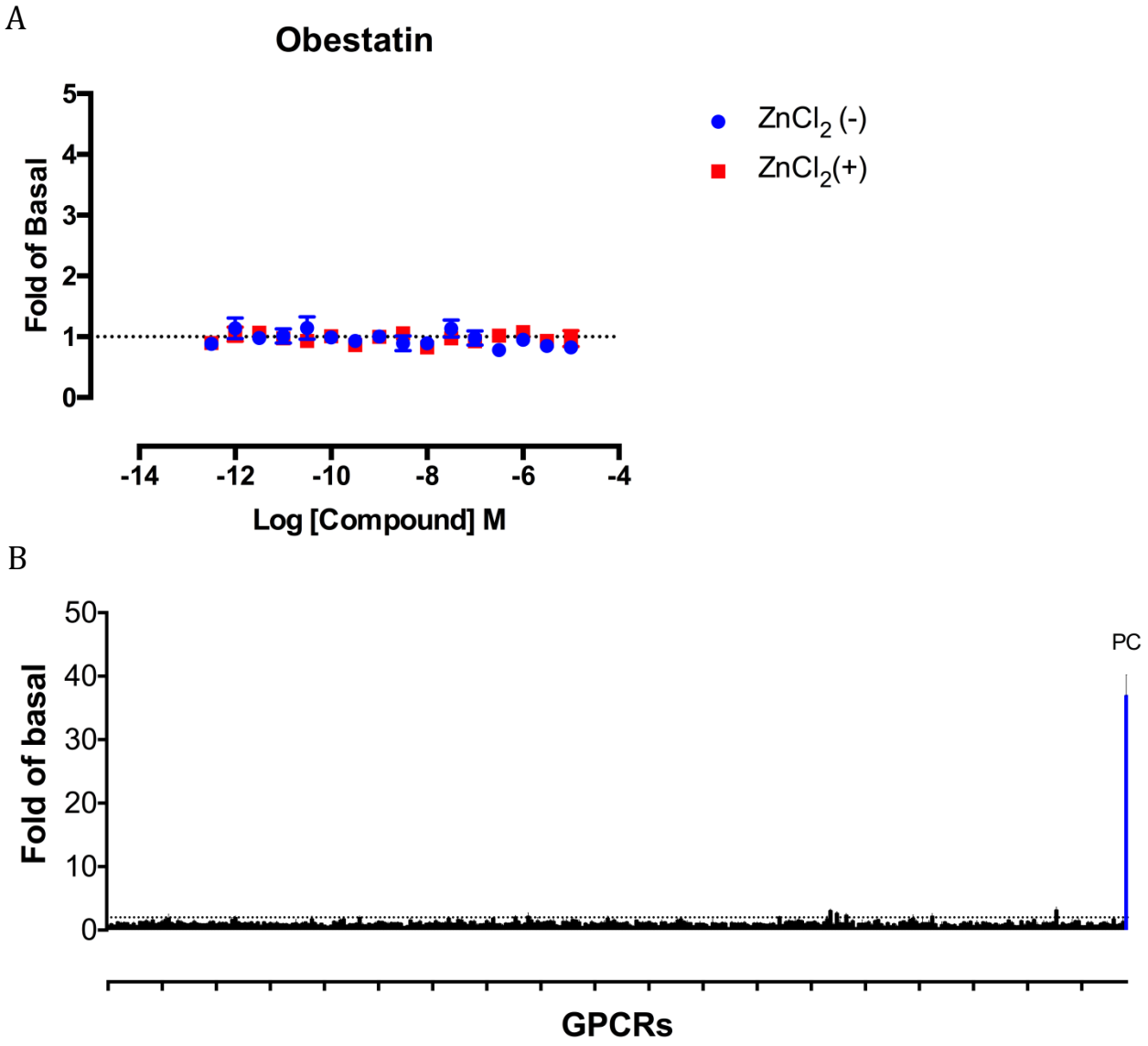

Supplementary Figure 1. (A) Lack of GPR39-dependent β-arrestin recruitment response to obestatin in TANGO assay with 100 μM $ZnCl_2$ or without $ZnCl_2$. This experiment was performed in quadruplicate. (B) GPCRome β-arrestin recruitment in response to obestatin as measured by the TANGO assay, performed using 1 μM obestatin with 100 μM $ZnCl_2$. The results are the mean ± S.E.M of quadruplicate determinations. PC (blue); Positive control, 1 μM quinpirole at DRD2.

Supplementary Figure 2

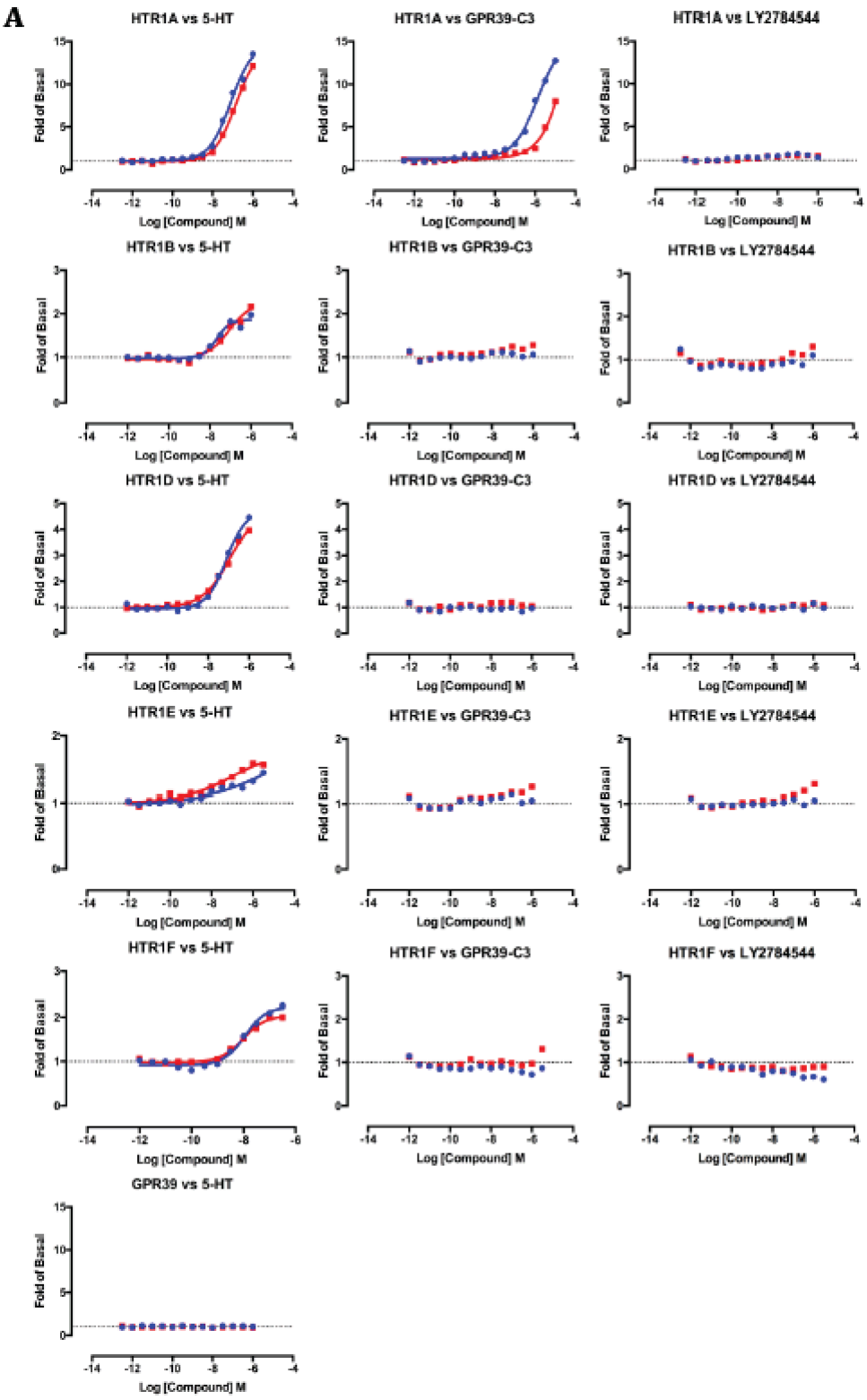

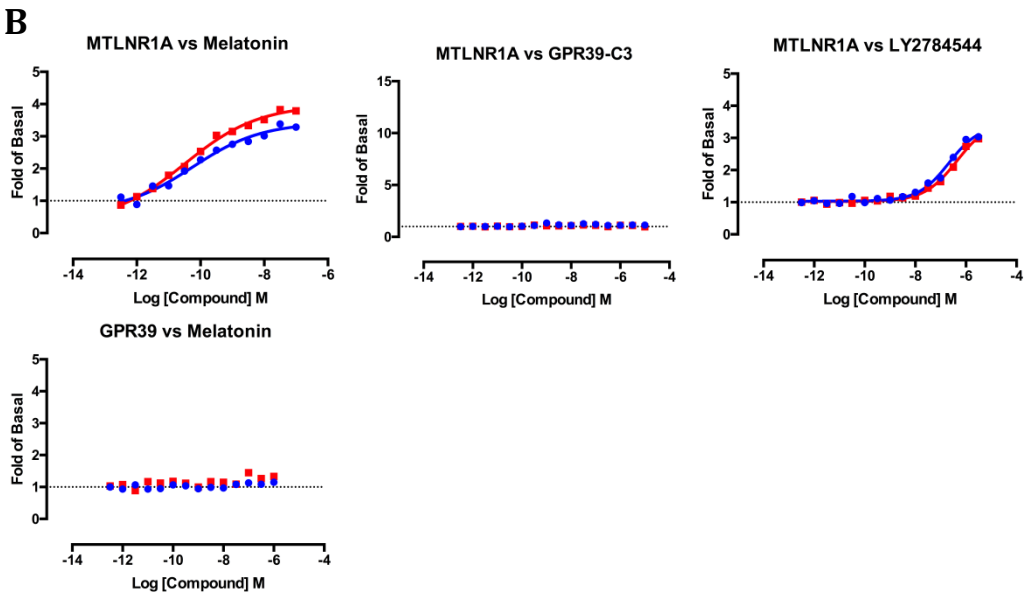

Supplementary Figure 2. Concentration-response curves showing β-arrestin recruitment responses to two GPR39 agonists to non-GPR39 targets as measured in the TANGO assay. (A) GPR39-C3 (middle panels) stimulates a response at HTR1A, but not at other 5-HT1 subfamily receptors; LY2784544 (right panels) is inactive at all 5-HT1 subfamily receptors. Positive controls with 5-HT are shown in the left panels. The bottom panel shows that 5-HT is inactive at GPR39. (B) LY2784544 (right panel) stimulates a response at MTLNR1A melatonin receptors, but GPR39-C3 (middle panel) does not; positive control with melatonin is shown in the left panel, and the bottom panel shows that melatonin is inactive at GPR39. Blue points and curves show experiments done in the presence of 100 μM $ZnCl_2$, and red points and curves show experiments done in the absence of $ZnCl_2$.

Supplementary Figure 3

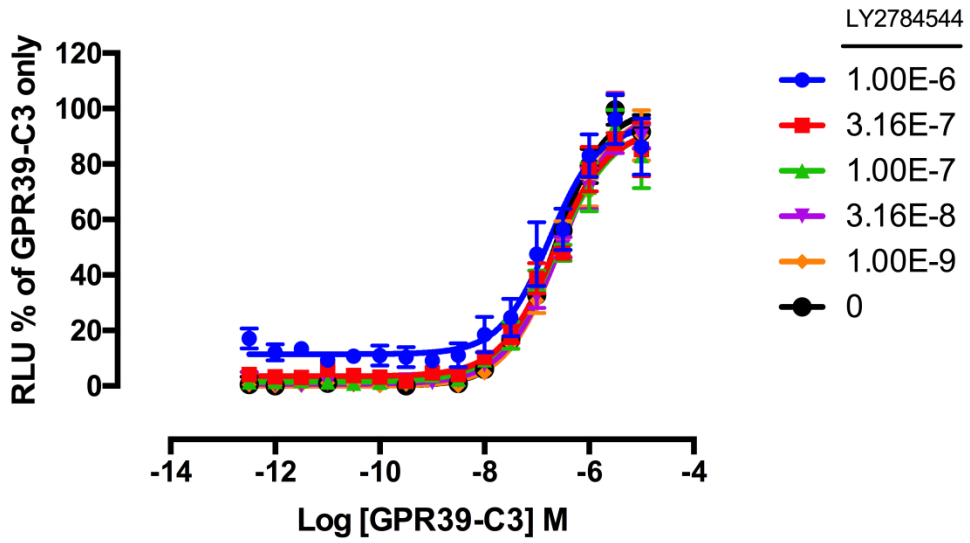

Supplementary Figure 3. Antagonist-mode β-arrestin recruitment measured using the TANGO assay, showing that various concentrations of LY2784544 do not block GPR39-mediated responses to GPR39-C3, done in the absence of Zn^{2+}. Values were normalized using the GPR39-C3 response as 0% (basal) to 100% (Emax). This experiment was performed in quadruplicate.

Supplementary Figure 4

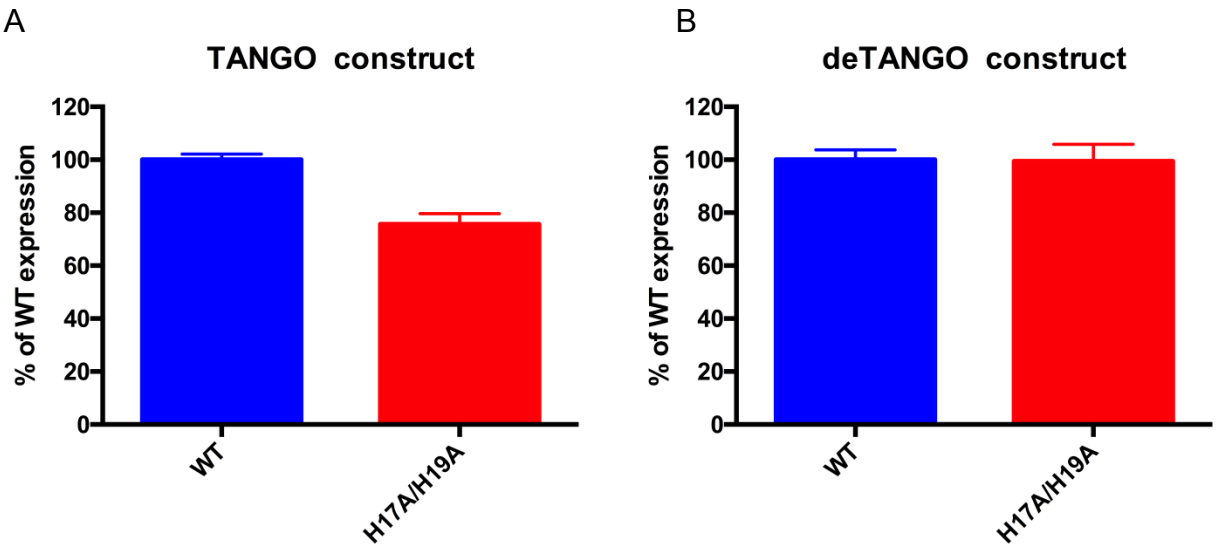

Supplementary Figure 4. Cell surface expression levels of GPR39 constructs and mutants in HEK293T cells. (A) TANGO constructs and (B) “deTANGOized” constructs. Cell surface expression levels were measured by Cell ELISA (methods). The results are the mean ± S.E.M. of at three independent experiments performed in quadruplicate.

Supplementary Figure 5

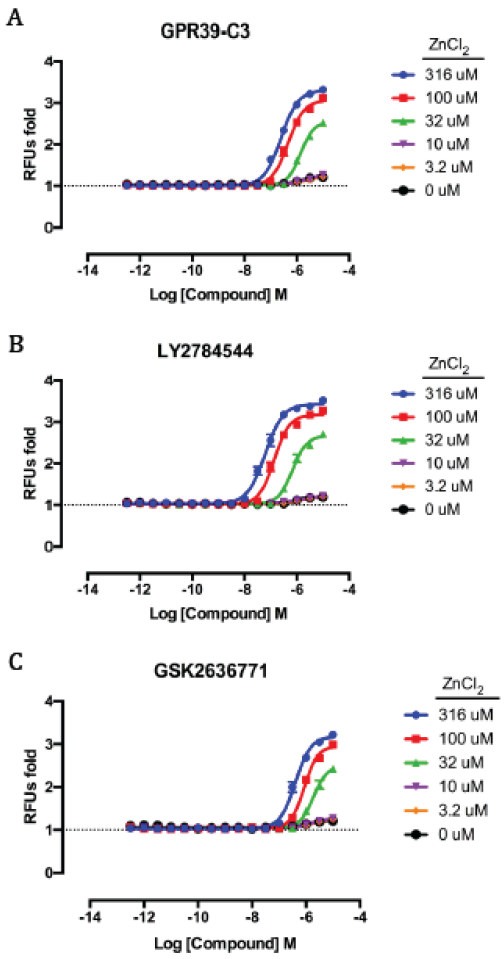

Supplementary Figure 5. Ca^{2+} influx response to GPR39-C3 (A), LY2784544 (B) or GSK2636771 (C) with various concentrations of $ZnCl_2$ in HT-29 cells. The results are the mean ± S.E.M. of at least three independent experiments performed in quadruplicate.

Supplementary Figure 6

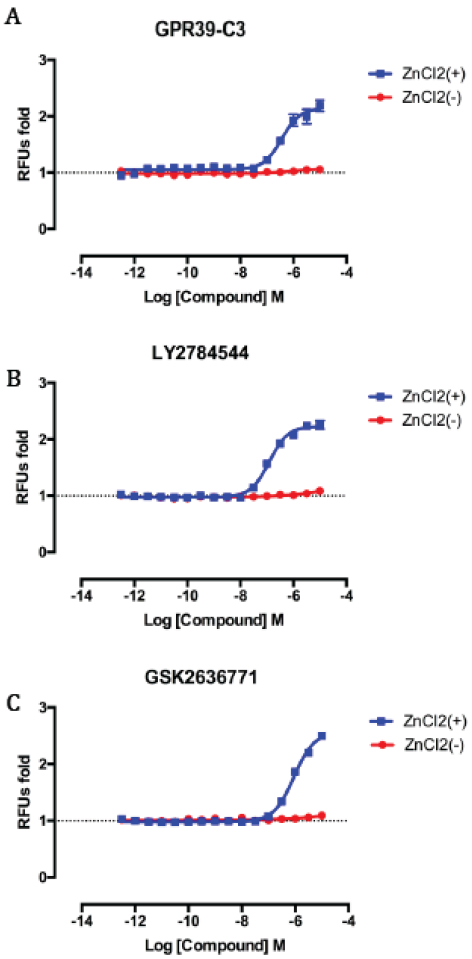

Supplementary Figure 6. Ca^{2+} influx response to GPR39-C3 (A), LY2784544 (B) or GSK2636771 (C) with 100 μM $ZnCl_2$ or without $ZnCl_2$ in PC-3 cells. The results are the mean ± S.E.M. of at two independent experiments performed in quadruplicate.